



UNIVERSITÀ POLITECNICA DELLE MARCHE

DIPARTIMENTO SCIENZE DELLA VITA E DELL'AMBIENTE

**Corso di Laurea Magistrale
Biologia Molecolare e Applicata**

Effetti dello stress ossidativo sullo sviluppo embrionale di *Danio rerio*

Oxidative stress effects on embryo development in *Danio rerio*

Tesi di Laurea Magistrale di:
Mariangela Di Vincenzo

Relatore Chiar.mo:
Oliana Carnevali

Correlatore:
Andrea Pessina

Sessione Autunnale

Anno Accademico 2018/2019

*A mio fratello Michele,
Qualunque cosa tu possa fare,
qualunque sogno tu possa sognare, comincia.
L'audacia reca in sé genialità, magia e forza.*

Comincia ora.

(Johan Wolfgang von Goethe)

ABSTRACT

Zebrafish, *Danio rerio*, è un piccolo teleosteo d'acqua dolce che grazie alle sue caratteristiche morfologiche, fisiologiche e genetiche è divenuto negli ultimi anni uno dei modelli sperimentali più utilizzati nel campo della ricerca. Abbiamo utilizzato *Danio rerio* per verificare l'efficacia della somministrazione della polidatina su processi infiammatori, ossidativi e rigenerativi. La polidatina è un polifenolo che possiede numerose proprietà benefiche, tra cui, proprietà antinfiammatorie e antiossidanti, inoltre abbiamo voluto testare la sua efficacia, preventiva o curativa in seguito a danni indotti da stress chimico mediante CuSO_4 o da stress meccanico mediante taglio della pinna caudale. L'eccesso di rame nelle cellule induce la formazione di una quantità eccessiva di ROS con conseguente danno ossidativo della cellula, che attiva meccanismi di difesa quali l'attivazione della risposta immunitaria, caratterizzata dall'espressione di citochine e migrazione leucocitaria, l'espressione di molecole antiossidanti e di riparazione della cellula mediante processi autofagici o di eliminazione della cellula attraverso processi apoptotici.

Il nostro studio ha rivelato che la polidatina riduce gli effetti infiammatori come evidenziato dai bassi livelli di *il1* e *il8* con conseguente minor migrazione di neutrofili nel sito di danno. Inoltre, abbiamo osservato che la polidatina

permette un incremento dell'espressione di geni con attività antiossidante quali *sod1*, *sod2* e *cat*. La polidatina permette un recupero della cellula anche mediante l'attivazione di processi autofagici, ma, allo stesso tempo, è responsabile anche dell'incremento dell'espressione del gene *cyclin b*, coinvolto nella proliferazione cellulare. L'esposizione a CuSO_4 delle larve di zebrafish induce necrosi delle cellule ciliate della linea laterale, la somministrazione della polidatina in concentrazioni di $400\mu\text{M}$ prima dell'esposizione al solfato di rame non previene in alcun modo la distruzione delle cellule ciliate, ma, potrebbe essere coinvolta in un miglioramento del processo rigenerativo mediante l'incremento dei geni *cldn b* e *phoenix* che codificano per fattori coinvolti nella rigenerazione cellulare. Analisi della morfologia hanno invece evidenziato che l'esposizione a CuSO_4 impedisce un corretto sviluppo della vescica natatoria, blocca la crescita della larva in termini di lunghezza e induce scoliosi nella larva. La polidatina permette un recupero dello sviluppo, e della crescita della larva in seguito all'esposizione al solfato di rame. La maggior parte dei risultati ottenuti indica che la polidatina ha un maggiore effetto se somministrata in seguito all'induzione del danno, quindi, ha una maggior efficacia se somministrata in maniera curativa piuttosto che preventiva.

ABSTRACT

Zebrafish, *Danio rerio*, is a small freshwater teleost that thanks to its morphological, physiological and genetic characteristics has become one of the most used experimental models in the field of research in recent years. We used *Danio rerio* to verify the efficacy of polydatin administration on inflammatory, oxidative and regenerative processes. Polydatin is a polyphenol that has many beneficial properties, including anti-inflammatory and antioxidant properties and we wanted to test its effectiveness, preventive or curative, in chemical stress induced by CuSO₄ or mechanical stress by cutting the caudal fin. The excess of copper in the cells allows the formation of high amount of ROS with consequent oxidative damage of the cell, which activates defense mechanisms such as immune response activation, characterized by the expression of cytokines and leukocyte migration, the expression of antioxidant and cell repair molecules through autophagic processes, when not possible, cells will die by apoptotic process. Our study revealed that polydatin attenuate the inflammation process as evidenced by the lower levels of *il1* and *il8* resulting in less migration of neutrophils to the site of damage. Furthermore, we have seen that polydatin allows an increase in the expression of genes codifying for enzymes involved in antioxidant activity such as *sod1*, *sod2* and *cat*. Polydatin allows a recovery of the cell also through the activation of autophagic processes, but, at

the same time, it is also responsible for the increase of the *cyclin b* gene, involved in cell proliferation. Exposure to CuSO₄ of zebrafish larvae induces necrosis of the lateral line hair cells, the administration of polydatin in concentrations of 400µM before exposure to copper sulphate has not preventive action on the destruction of the hair cells, but it could be involved in an improvement of the regenerative process by also increasing the *cldn b* and *phoenix* genes when provided after CuSO₄ exposure. Morphology analysis has shown that exposure to CuSO₄ prevents the correct development of the swim bladder, blocks larva growth in terms of length and induces a dorsal curvature (Scoliosis), interestingly polydatin allows a recovery of development and growth. Most of the results obtained indicate that polydatin has a greater effect if given following damage induction, therefore, it is more effective if administered in a curative rather than a preventive manner.

INDEX

1. <u>INTRODUCTION</u>	1
1.1 <i>Danio rerio</i> as organism model	1
1.1.1 General features.....	1
1.1.2 <i>Danio rerio</i> like the Roman God Janus.....	3
1.1.3 A model for study Innate Immune System.....	4
1.1.4 Zebrafish as a model for tissue regeneration.....	6
1.2 Polydatin	10
1.2.1 Polydatin chemical properties and pharmacokinetics.....	12
1.2.2 Beneficial and pharmacological effects.....	13
1.2.3 PD in zebrafish.....	17
1.3 Copper metabolism and dysregulation.....	18
1.3.1 Copper excess induces inflammation and other reparative processes in the cell through ROS production	21
1.3.2 Copper exposure induce inflammation and neuromast death in zebrafish larvae.....	27
1.4 Genes analyzed.....	30
2. <u>RESEARCH OBJECTIVE</u>	37
3. <u>MATERIALS AND METHODS</u>	38
3.1 Tanks set up, coupling, collecting and maintaining embryos.....	38
3.2 Experimental design.....	39
3.3 Morphological analysis.....	44

3.3.1	Length measurement.....	44
3.3.2	Swim bladder development and dorsal curvature.....	44
3.4	Myeloperoxidase (MPO) test.....	45
3.4.1	Sampling time test after copper sulfate exposure.....	46
3.4.2	Polydatin treatment timing test.....	47
3.5	DASPEI staining.....	49
3.6	Semi-quantitative Real-time PCR (RT-PCR) analysis.....	50
3.6.1	Sampling.....	50
3.6.2	RNA extraction.....	50
3.6.3	Electrophoresis gel.....	52
3.6.4	DNase treatment.....	54
3.6.5	Reverse transcription.....	54
3.6.6	Semi-quantitative RT-PCR.....	55
3.7	Statistic analysis.....	57
4.	<u>RESULTS</u>	58
4.1	Morphological analysis.....	58
4.1.1	Length measurement.....	59
4.1.2	Swim bladder development and dorsal curvature.....	61
4.2	MPO TEST.....	63
4.2.1	Sampling time test after copper sulfate exposure.....	63
4.2.2	Polydatin treatment timing test.....	64
4.2.3	MPO TEST – CuSO ₄ experiment.....	67
4.2.4	MPO TEST- Cut tail experiment.....	70

4.3	DASPEI STAINING	71
4.4	Semiquantitative RT-PCR.....	73
4.4.1	Inflammation pathway.....	73
4.4.2	Oxidative stress pathway.....	75
4.4.3	Apoptosis and autophagy pathway.....	77
4.4.4	Neuromast regeneration pathway.....	80
4.4.5	Proliferation pathway.....	82
5.	<u>DISCUSSION</u>	84
6.	<u>CONCLUSIONS AND FUTURE PERSPECTIVES</u>	92
	<u>BIBLIOGRAPHY</u>	93
	<u>INDEX OF FIGURES</u>	105
	RINGRAZIAMENTI	

1. INTRODUCTION

1.1 *Danio rerio* as organism model

Zebrafish, *Danio rerio* (Hamilton, 1822), was first described by Francis Hamilton in the early nineteenth century and in the last 40 years it has become one of the most widely used model organisms for scientific research in vertebrate including development, genetics, tissue regeneration and toxicology (Simonetti et al., 2015).

1.1.1 General features

Zebrafish (*Danio rerio*) is a omnivorous freshwater teleost fish native to Southeast Asia, belonging to the Cyprinids family and the Actinopterygii class (rayed fin fish; Lawrence, 2007)

Danio rerio has a fusiform body, laterally compressed and characterized by the presence of dark blue longitudinal strips extending from behind the operculum to the caudal fin.



Fig.1.1 Females and male zebrafish. (www.asianscientist.com)

Zebrafish reproduction occurs at dawn, in shallow waters (Engeszer et al., 2007; Spence, Ashton and Smith, 2007). It shows courting behaviors that lead to eggs release by the female and sperm by the male in a coordinated manner with consequent fertilization (Darrow and Harris, 2004). Zebrafish embryonic development is rapid at temperatures around 28°C and chorion transparency allows the observation and the study of the embryogenesis processes very easily (Kimmel et al., 1995).

Hatching occurs between 48h and 72h post fertilization (3 days post fertilization, dpf) and marks the end of the embryonic period. Larvae, immediately after hatching, have a size of about 3mm, and attach themselves to hard surfaces through secretory cells located in the epidermis of the head (Laale, 1977) and through a series of attachments as they reach higher levels air-water boundary where they swallow an air bolus to inflate the developing swim bladder (an hydrostatic organ, Goolish et al., 1999). In the days following

hatching the larvae consume the nutrients present in the yolk sac until the mouth is opened, about at 5dpf (Fraher et al., 2016).

Four weeks after hatching, zebrafish reach a size around 11mm and it enters in a juvenile stage; in this stage sex can be distinguished with certainty only through organ dissection. They reach sexual maturity about 10-12 weeks after hatching and females can be easily recognized thanks to their more rounded shape in correspondence of the ovary and by the presence of a small genital papilla in front of anal fin. Adult males have a larger anal fin and a color that tends to yellow (Parichy et al., 2009). Zebrafish sexual determination mechanisms are not yet fully understood, although it is known that it is not based on the inheritance of sex chromosomes, but it is probably determined by environmental factors and/or a polygenic sex determination system (Liew and Orbán, 2014).

1.1.2 *Danio rerio* like the Roman God Janus

Mariotti et al. (2015) compared *Danio rerio* to Roman God Janus, often a deity with two faces, capable to look into the past and the future, and inside and out of the house door. Similarly, Zebrafish is an “old” experimental model that allows to look at the future, thanks to its "double face"; encloses two models in one: larval stage and adult stage (Mariotti et al., 2015). Furthermore, optical transparency of zebrafish embryos and larvae makes them ideal for microscopic

imaging of vital processes and allows the use of fluorescent markers to "illuminate" different cells and organs "inside and out" organism.

The first to use zebrafish as an experimental model were George Streisinger and Kimmel in the 1970s, they conduct research on developmental biology, in particular: embryonic development, nervous system, muscular system and regulation of gene expression.

The robustness and the possibility to be farmed and manipulated more easily than other animal models, e.g. mouse (*Mus musculus*) have promoted the use of *Danio rerio* as experimental animal model (Simonetti et al., 2015)

One of the most important features of zebrafish is its evolutionary proximity to humans; in fact, about 70% of the genes involved in human pathologies have functional counterparts in zebrafish. This allowed us to use zebrafish to study the processes that are involved in development and pathogenesis, such as, for example, angiogenesis, the development of the enteric nervous system, tumorigenesis and pharmacotoxicity (Khan and Alhewairini, 2018).

1.1.3 A model for study Innate Immune System

After hatching larvae can be exposed to the external environment right away; therefore, the innate immune system must be present from day 1 after fertilization (Herbomel et al., 1999, 2001). On the other hand, the adaptive

immune system develops completely just 4-6 weeks after fertilization when lymphocytes become functional (Willett et. al., 1999; Lieschke and Currie, 2007). The transparency of the embryonic stage and this temporal difference in the development of the 2 immune systems allows the use of zebrafish as a study model for the inborn immune response *in vivo* regardless of the adaptive one (Novoa et al., 2012).

Immune response activation is produced by a series of mechanisms that, in a coordinated way, activate different cellular populations and secretion of different molecules, with the aim of eliminating the foreign agent.

Damaged cells release endogenous molecules, such as cytokines and pro-inflammatory chemokines, capable of triggering an acute inflammatory response (Kono and Rock, 2008). IL-1 β (Interleukin-1 β), TNF α (Tumor Necrosis Factor alpha), IL-6 (Interleukin 6) and IL-8 (Interleukin 8) are the main proinflammatory mediators that have the ability to recall the cells of the immune system at the site of damage (Mocchegiani et al., 2014; Malavolta et al., 2015; Fischer and Maier, 2015). The first innate immune system cells to migrate to the site of infection are neutrophils, a type of leukocytes (Novoa, 2011) that will later be replaced by macrophages able to phagocyte tissue debris and bacterial cells (Martin and Leibovich, 2005). This has been confirmed by Li et al., 2012, who have observed that after caudal fin amputation the first cells

to migrate towards and swallow the debris of the damaged cells were neutrophils. Unfortunately, neutrophils phagocytic capacity is limited and they could swallow less than four pieces of cellular debris, therefore, about 20 minutes later, these neutrophils underwent a series of morphological alterations that resembled the characteristics of apoptosis, including membrane blebbing, chromatin condensation and nuclear fragmentation. Six hours after tail amputation macrophages arrived and began to gobble up the rest of the debris and apoptotic neutrophils. The caudal fin begins a regeneration process about 12 hours after the lesion and it ends after about 4-5 days. During this time the macrophages were dominantly placed at the site of damage, suggesting their involvement in the repair and proliferation mechanisms of the caudal fin cells (Li, Li et al., 2012).

1.1.4 Zebrafish as a model for tissue regeneration

Recently, zebrafish has been used to study the behaviour of stem cells and the processes that regulate tissue regeneration in vertebrates. In fact, Zebrafish has the ability to regenerate various tissues that have suffered an injury, such as the caudal fin, heart, liver, kidneys, central nervous system and hair cells of the lateral line (Gemberling et al. 2013).

Aquatic vertebrates, such as amphibians and teleosts, are characterized by the presence of a lateral line. Lateral line is a sensory system consisting of mechanoreceptors, called neuromasts. The lateral line system allows to detect the direction, density and direction of the wave motions.

In zebrafish, the lateral line consists of two main components, an anterior lateral line consisting of the neuromasts of the head, maxilla and operculum and a lateral posterior line formed by the neuromasts of the trunk and tail (Gompel et al., 2001). During embryonic development neuromasts are progressively added along the lateral line thanks to some progenitor cells called Primordium. Lateral line development begins 48 hours post fertilization (hpf) with the addition of the first anterior lateral line neuromasts. Subsequently the first neuromasts of the posterior lateral line appear, L1 and L2, followed by the neuromasts L3, L4 and L5 perfectly spaced. Finally, there is the addition of the neuromasts L6, L7 and L8 grouped at level of the tail (Ledent, 2002).

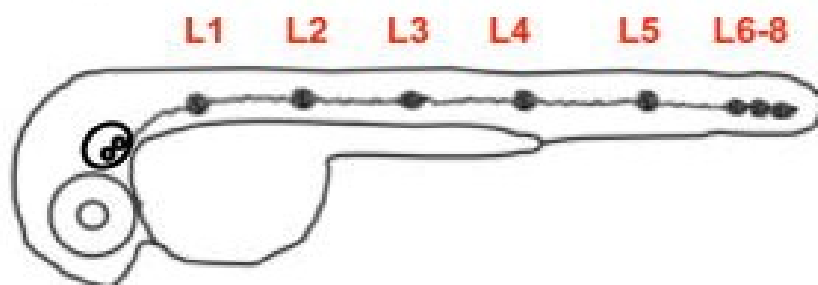


Fig.1.2 Posterior lateral line neuromasts at 3dpf. (Chitnis et al., 2012).

During larval development the number of neuromasts increases, the lateral line of an adult zebrafish can also be made up of over 60 neuromasts (Nuñez et al., 2009).

Neuromasts are made up of several types of cells: hair cells, support cells and mantle cells (Williams and Holder, 2000). The number of hair cells can vary according to the size of the neuromast and can vary from dozens to thousands. In the basal part of the hair cells there are synaptic contacts with afferent and efferent nerve fibers that allow the transmission and reception of nerve signals. Stereocilia of the hair cells are immersed in a cupula formed by a gelatinous medium secreted by the supporting cells (Haehnel et al., 2012).

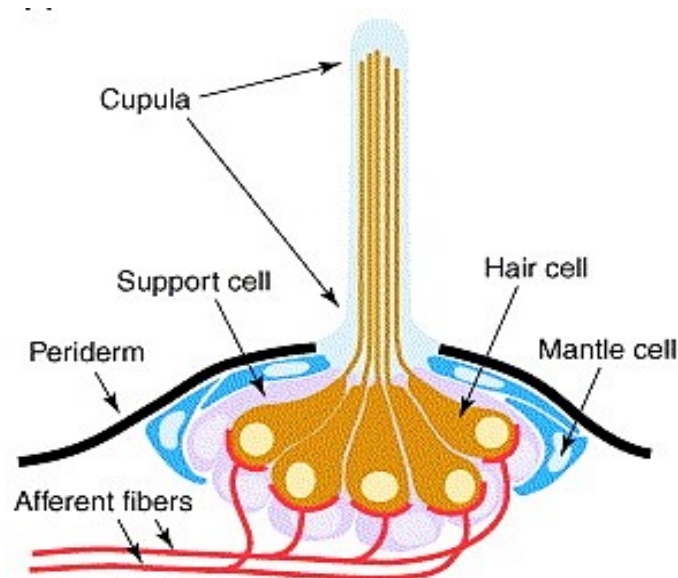


Fig1.3 Neuromast structure (Ghysen and Dambly-Chaudière, 2004).

The hair cells of neuromasts are similar to hair cells present in the inner ear of mammals, which are receptors responsible for detecting head movements and sounds (Nicolson, 2017). Several environmental factors, such as noise pollution, the use of some antibiotics or anti-cancer drugs are responsible for damaging the hair cells of the inner ear (Campo et al., 2013). Likewise, many studies have been conducted in which it has been shown that exposure to neomycin (Harris et al., 2003), to heavy metals (Hernandez et al., 2007), to UV rays (Gompel et al., 2001) can damage the hair cells of neuromasts. Neuromasts that have suffered damage have the ability to regenerate hair cells; time-lapse imaging experiments show that regeneration of hair cells in the lateral line is achieved through the induction of proliferation and the subsequent differentiation of internal support cells (Lopez-Schier and Hudspeth, 2006; Ma et al., 2008; Mackenzie and Raible, 2012; Wibowo et al., 2011). However, the mechanism that allow the regeneration of these cells are not yet well understood. It is thought that the hair cell matures through cell-to-cell contact and/or expression of an inhibitory signal blocks proliferation and differentiation of support cells. Therefore, damage to the hair cells would lead to the reactivation of these processes in the supporting cells (Bergmann and Steller, 2010). In recent years, creation of transgenic lines has contributed greatly to the study of the expression of genes involved in these processes, but

much progress has yet to be made; e.g Phoenix is a protein expressed only in the supporting cells of neuromasts whose function is not yet known. *phoenix* mutants have a normal develop; but they fail to completely regenerate damaged hair cells. This regeneration deficiency affects only the hair cells, as it has been seen that in phoenix mutants that had undergone caudal fin amputation regeneration normally occurred (Behra et al., 2009).

1.2 Polydatin

Polydatin (PD or PLD), also called piceide (or (*E*)-piceid, (*E*)-polydatin, *trans*-polydatin, 3,4',5-trihydroxystilbene-3- β -d-glucoside), is a monocrystalline substance that is extracted from the roots and rhizomes of *Polygonum cuspidatum*, a plant native to East Asia.



Fig.1.4 *Polygonum cuspidatum* (www.zeauiverse.com).

This plant is also called "false bamboo" for its hollow stems with different relief nodes. It has been used historically in traditional Chinese medicine as an analgesic, antipyretic, diuretic and expectorant (Du et al., 2013). Today it is known that the beneficial properties of this plant are due to the high concentration of polyphenols. More than 8000 polyphenolic compounds have been identified, they are natural organic molecules produced from the secondary metabolism of fruit, vegetables, cereals and their derivatives. Polyphenols are involved in defences against UV radiation and/or pathogens in plants (Pandey and Rizvi, 2009); they generally derive from phenylalanine and they occur in forms conjugated with mono or polysaccharides. Based on the chemical characteristics of the polyphenolic compound, these are divided into 4 main classes: phenolic acids, flavonoids, stilbenes and lignans.

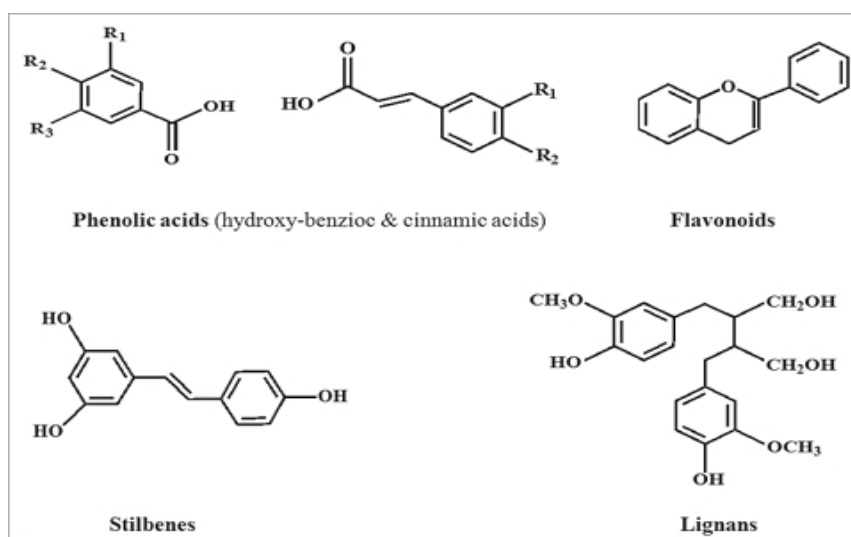


Fig.1.5 Chemical structures of the different classes of polyphenols (Pandey and Rizvi, 2009).

In the last decade polyphenols have become of great scientific interest thanks to discovery of their numerous beneficial properties, one of the most studied stilbenes thanks to its abundance and its multiple properties is polydatin.

1.2.1 Polydatin chemical properties and pharmacokinetics

Polydatin is a polyphenol analogous to resveratrol, the main differences lie in their chemical structure; in fact, resveratrol has a hydroxyl group linked to carbon C3, while polydatin represents the glycosylated form of resveratrol, as it replaces the hydroxyl group with a glucosidic group.

Both resveratrol and polydatin exists in trans and cis conformations, but the bioactivity of the trans conformations are higher than the cis conformations (Mikulski and Molski, 2010).

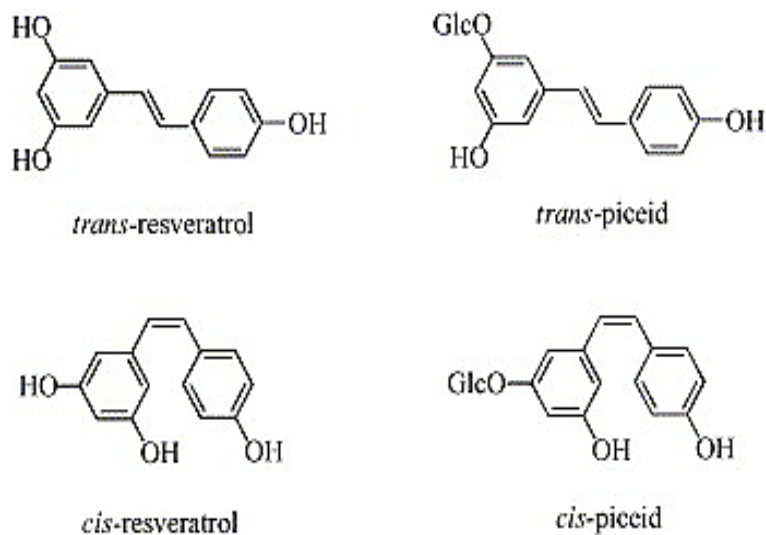


Fig.1.6 Resveratrol and polydatin cis and trans conformations (Vian et al., 2005).

In particular, polydatin has greater efficacy than resveratrol due to its chemical structure, in fact, the glucosidic group in position C3 makes the molecule of polydatin more soluble in water, more resistant to enzymatic attacks and it improves its absorption by tissues through glucose transport mechanisms (Henry et al., 2006).

In fact, unlike the resveratrol which enters in cell through a passive transport mechanism, the polydatin enters in cell via Sodium-GLUcose Transporter (SGLT1), a transmembrane protein that allows the transport of glucose by exploiting the electrochemical gradient of sodium (Henry et al., 2005).

All these features make it an optimal substitute for resveratrol as a therapeutic substance.

1.2.2 Beneficial and pharmacological effects

Thanks to its ability to be totally absorbed by the body, its solubility and its stability, polydatin has become, in recent years, a substance of pharmacological interest. Various studies show the beneficial and pharmacological properties of polydatin are reported in the Fig.1.7:

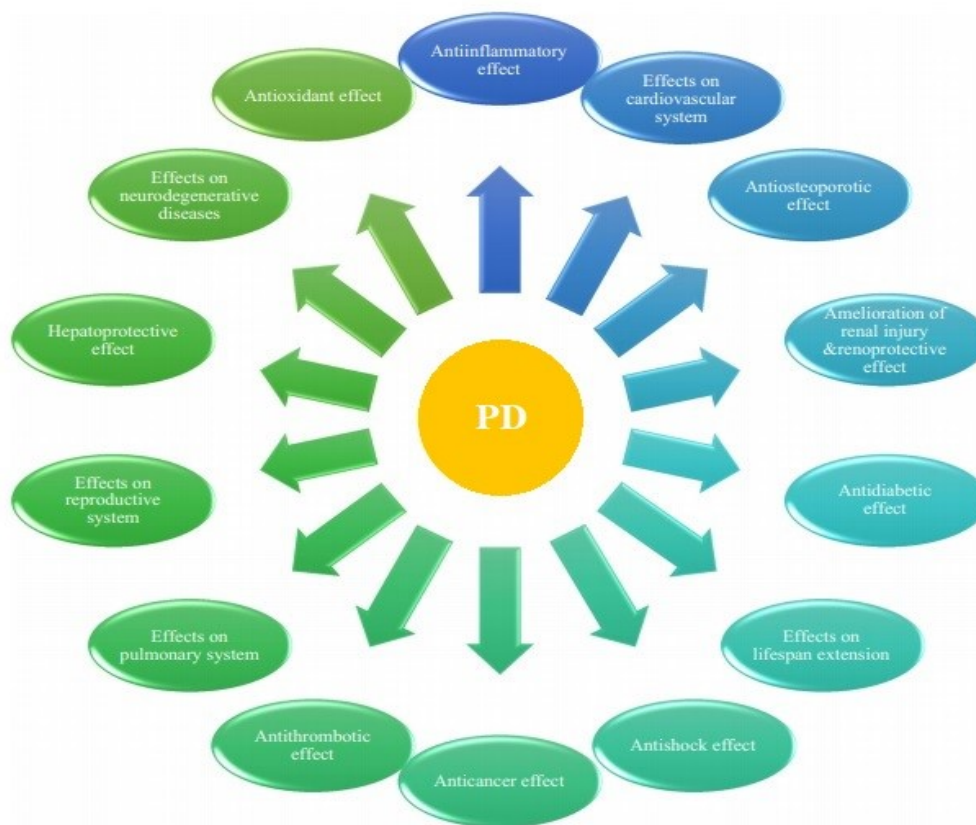


Fig.1.7 Biological properties of PD

Biological proprieties of PD are summarized by Şöhretoğlu et al., 2018.

- **Antioxidant Activity:** like other polyphenols also polydatin has high antioxidant properties. Studies conducted by He et al. in 2012 showed that PD decreases death and free radical production in HaCat cells subjected to UV radiation. Furthermore, PD has a slower but more prolonged protective action against lipid peroxidation and is much more effective than resveratrol (Fabris et al., 2008). In mice in which was induced oxidative stress, oral administration of PD and resveratrol allowed a more effective response to oxidative damage by increasing

SOD (Superoxide dismutase) and CAT (Catalase) activity (Wang et al. 2015).

- **Anti-Inflammatory Activity:** numerous studies have shown that polydatin is able to modulate cytokines expression involved in inflammatory processes. Ravagnan et al. in 2013 demonstrated that, in human keratinocytes subjected to thermal stress, PD is able to regulate the gene expression of *il6* (*interleukin 6*), *il8* (*interleukin 8*) and *tnfa* (*tumor necrosis factor α*) and allowed an overproduction of HSP70 (Heat shock proteins 70 kilodalton), a protein with cyto-protective activity and involved in cell and tissue repair.
- **Anti-Tumor Activity:** many studies have shown that PD possesses cytotoxic effects against some human tumor cell lines such as CNE nasopharyngeal carcinoma cells, HeLA human cervical carcinoma cells, SMMC-7721 cells of hepatoma cells and A-431 carcinoma cells epidermal (Liu et al., 2011). It has also been seen that PD has a greater affinity with G-quadruplex, a rich in guanine portion of VEGF promoter (vascular endothelial growth factor) involved in proliferation of tumor cells. PD binds to G-quadruplex and blocks VEGF transcription (Balasubramanian and Neidle, 2009; Li and Yuan, 2010; Sun et al., 2005). Have also been conducted *in vivo* studies to assess the ability of

PD to mitigate the side effects of chemo and radio therapy and the cases evaluated reported improvements during therapy (Bonucci et al., 2018).

- **Antimicrobial Activity:** PD with other substances extracted from the root of *P. cuspidatum* reduces the production of glycolytic acid and glucosyltransferase by *S. mutans* and *S. sobrinus* that induce the development of dental caries (Ban et al., 2010).
- **Protective Effects on Myocardial Cells:** numerous studies have been conducted to evaluate PD effects on cardiocytes. In fact, PD can reduce toxicity induced by adriamycin in rat cardiocytes (Zhao et al., 2010). Furthermore, it has been seen that in myocardial infarction, PD decreases the ischemic and infarcted area, reduces lactate dehydrogenase (LDH) and creatine kinase (CK) activity, and therefore relieves ischemic lesion of cardiomyocytes (Zhang et al., 2006).
- **Hepatoprotective Effects:** several studies indicate that PD can reduce liver damage induced by high fat intake and carbon tetrachloride (CCl₄) (Huang et al., 1999). Other studies indicate that under fasting conditions polydatin reduces insulin, glucose and TNF α levels in serum and improves the insulin sensitivity index (Zhang and Lv, 2010).

- **Neuroprotective Effects:** PD has neuroprotective activity too. In fact, it can protect from brain damage caused by the permanent occlusion of the middle cerebral artery (Ji et al., 2012), it can attenuate cognitive deficits caused by chronic cerebral hypoperfusion (Li et al., 2012) and can improve learning abilities in mice with chronic alcoholism (Xu et al., 2011, 2012). It was also seen that PD is able to alleviate the neurodegenerative effects involved in Parkinson's and Alzheimer's disease (Chen et al., 2015; Xiao et al. 2014).

1.2.3 PD in zebrafish

Danio rerio was used as experimental model even to evaluate the protective and pharmacological properties of PD. Lai et al. (2018) have shown that PD is able to alleviate liver injury induced by ethanol in zebrafish larvae. Excessive alcohol consumption leads to alcoholic liver disease (ALD) which includes a series of liver disorders including liver cirrhosis. In this study, zebrafish larvae were exposed to ethanol and subsequently treated with PD. It was seen that the it allowed a reduction of the oxidative stress, during the initial phases of liver damage, a downregulation of FASN that catalyzes long-chain fatty acids synthesis, and an apoptosis reduction through the downregulation of CHOP and GADD45 α .

Another study was conducted by Pardal et al. (2014) to evaluate the metabolization of resveratrol and PD and their ability to reduce lipid reserves in zebrafish larvae. Zebrafish larvae have a yolk sac that acts as a lipid reserve during embryonic development. This study showed that both resveratrol and PD allow a fat reserves reduction in a dose dependent manner.

Therefore, zebrafish proved to be a perfect experimental model for the study of the properties and efficacy of polyphenols in some pathologies.

1.3 Copper metabolism and dysregulation

Copper is a micronutrient introduced into the body through food and it is the third most abundant transition metal in humans with concentrations in the range of about 80-100mg (Pal, 2014; Hordyjewska et al., 2014).

Copper is essential for many biological processes as it is part of proteins involved in various metabolic functions, such as catalytic activities, proteins interactions and promoting structural changes (Kim et al., 2008). It is essential for the oxide-reduction reactions as it acts as a donor and electron acceptor (Mikolay et al., 2010), in fact, in some compounds copper exhibits an oxidation state Cu^{3+} or Cu^{4+} , but in biological systems copper ions are mainly Cu^+ or Cu^{2+} and for this reason it is an essential component of some enzymes with

antioxidant activity, such as copper-zinc superoxide dismutase enzyme (Cu/Zn SOD). The transition between oxidation states can generate hydroxyl radicals that can cause oxidative damage to biological macromolecules, this explains why copper can be highly toxic in concentrations higher than those required (Tisato et al., 2010). Copper concentrations are regulated by homeostasis which includes processes of absorption, transport, storage and excretion by the body (Gaetke et al., 2014). The absorption of copper takes place at the intestine level, where it enters the cells of the intestinal epithelium thanks to the membrane proteins, CTR1 (Kim et al., 2008). Within the intestinal cells, copper binds to albumin and other low molecular weight compounds and it is transported to the liver via portal circulation (Hordjeswska et al., 2014). CTR1 is also present in hepatocytes membranes and it allows the entry of copper into cytoplasm. Once in the hepatocytes, copper can be sequestered or by metallothioneins (MT) involved in detoxification of non-essential metals, or by glutathione (GSH) which has antioxidant activity. Furthermore, copper can be transported by chaperonins such as ATOX 1, which binds Cu^+ ion and transfers it to ATP7A and ATP7B. Both molecules are ATP dependent membrane transporters that allow the secretion of copper from the cell (La Fontaine et al., 2010). ATP7B transfers copper to ceruloplasmin (Cp), a protein that has the task of transporting about 90% of the copper in the blood. Another chaperonin is the

CCS (copper chaperone for superoxide dismutase) which allows the transfer of copper ions to SOD1 (Cu/Zn Superoxide Dismutase) an enzyme with a powerful antioxidant activity (Scheiber et al., 2013).

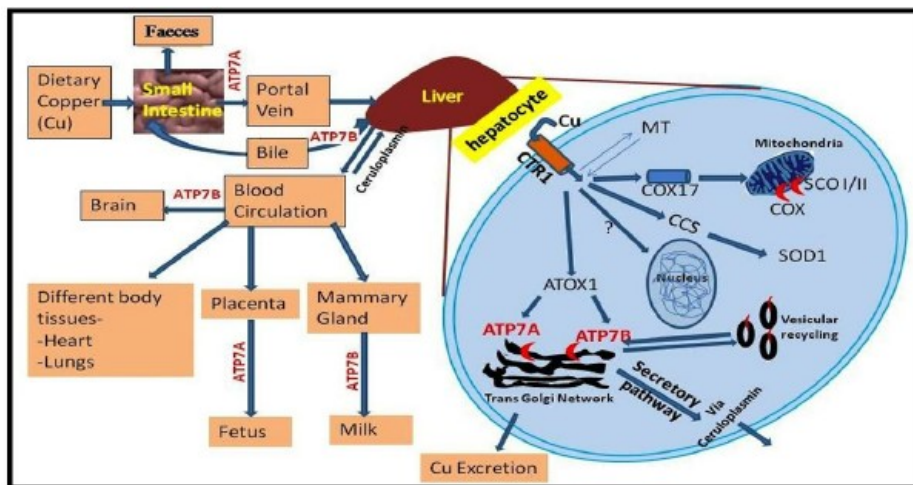


Fig.1.8 Copper metabolism (Rajendra Prasad and Sandeep Kumar, 2013).

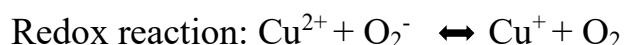
The use of copper pots or copper piping systems for drinking water, the intake of supplements and minerals or foods with high copper content can lead to excessive ingestion of copper with harmful effects on health.

Excess copper has been linked to the development of several neurodegenerative diseases. An imbalance of copper homeostasis has been associated with several physiological dysfunctions. For example, it has been seen that a copper deficiency can cause anemia, myopathy (Kumar et al., 2004), cognitive problems (Tan et al., 2006), myelopathy (Jaiser and Winston, 2010), Menkes disease and other neurological dysfunctions. On the contrary, an excess of copper inside the body has been associated with some serious

neurodegenerative diseases, such as Parkinson's, Huntington's, Alzheimer's diseases (Mocchegiani et al., 2012) and in addition to some hereditary disease such as Wilson's disease. Wilson syndrome, for example, is a genetic disease in which there is a mutation of ATP7B and a reduced expression of ceruloplasmin, this leads to an excessive accumulation of copper in the liver which can be fatal if it is not treated with anti-copper agents.

1.3.1 Copper excess induces inflammation and reparative processes in cell through ROS production

Copper can induce the activation of inflammatory process through reactive oxygen species (ROS) production by redox reactions and Fenton reaction (Romero et al., 2014):



The main ROS are: hydroxyl radicals ($\cdot\text{OH}$), peroxy radicals ($\text{ROO}\cdot$), alkoxy radicals ($\text{RO}\cdot$), superoxide anion ($\cdot\text{O}_2^-$) oxygen singlet ($^1\text{O}_2$) and hydrogen peroxide (H_2O_2). In addition to chemicals, such as CuSO_4 , ROS can be generated during cellular metabolism or by exposure to cigarette smoke, irradiation, air pollutants and ozone. To avoid damage to macromolecules present at high ROS concentration (Halliwell, 2011) cells can produce

molecules with antioxidant properties. However, when ROS production exceeds the cellular capacity of antioxidants, an oxidative stress occurs. A prolonged oxidative stress is responsible for several diseases of human inflammation (HID) and in extreme cases this can lead to cell death through processes such as apoptosis, necrosis and autophagy (Pallepati and Averill-Bates, 2012; Pantopoulos et al., 2012; Denton et al., 2018).

Inflammation is a response implemented by the immune system to protect the body from damage caused by external agents and promote tissue repair. High ROS production induces an immune response through activation of the transcription factor NF- κ B (Morgan et Liu, 2010). NF- κ B is a nuclear transcription factor that modulates genic expression in different cellular processes, such as the inflammatory response, cell proliferation, embryogenesis and apoptosis. The NF- κ B family of transcription factors consists of 5 proteins: p65 / RelA, RelB, c-Rel, p105/p50 (NF- κ B1) and p100/p52 (NF- κ B2) (Mitchell et al., 2016). These are associated with each other to form transcriptionally active homo and heterodimers. All 5 proteins possess an RHD domain that allows dimerization, DNA binding, interaction with I κ B and nuclear translocation.

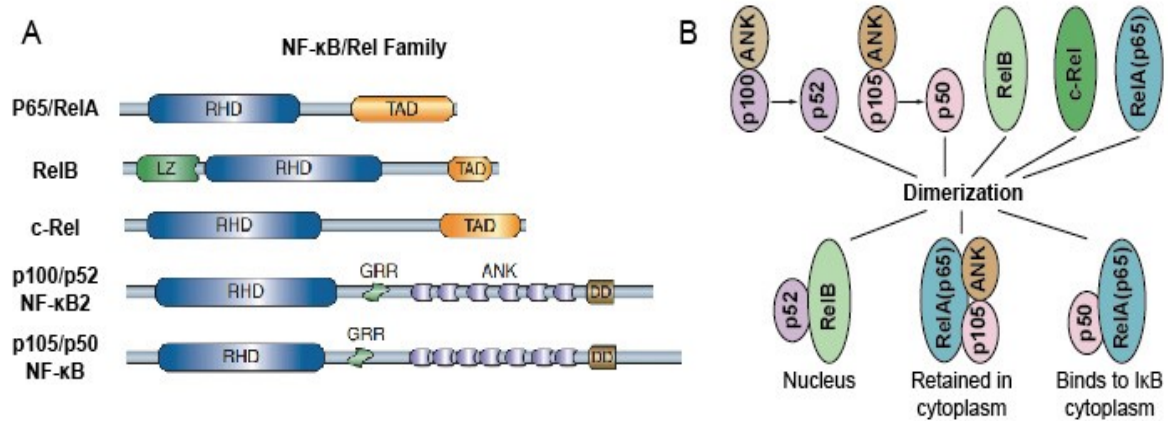


Fig.1.9 NF-κB Family (www.creative-diagnostics.com)

IκB is a family of inhibitory proteins consisting of IκBa, IκBb and IκBg that contain 6 repeats of ankyrin that allow binding to the RHD portion of the NF-κB proteins, inhibiting their function and keeping them in the cytoplasm. The activation of NF-κB by ROS leads to the dissociation of IKK from RHD domain with consequent translocation of NF-κB into the nucleus where it binds DNA (Lingappan, 2018). Binding of NF-κB with DNA promotes the transcription of various genes involved in different cell repair processes and in antioxidant activity. NF-κB promotes the transcription of cytokines, such as IL-1, IL-6, IL-8 and TNFα, which have the task of recruiting innate immunity cells at the site of injury. (Liu et al., 2017).

When cellular inflammation processes fail to be contained / contrasted by the cell, can be triggered the apoptosis process (Pallepati and Averill-Bates, 2012) and autophagy (Denton et al., 2018).

Apoptosis is characterized by the activation of cysteine-dependent aspartate proteases (caspases; Shalini et al., 2015). Caspases consist of upstream initiators such as caspases-8, -10, -2 and -9 and downstream effectors such as caspases-3, -6 and -7. Upstream of caspase activation apoptosis can be triggered by three main signaling pathways: death receptors located on the cell surface (Green and Llambi, 2015) or intrinsic pathways involving mitochondria or endoplasmic reticulum (ER; Ferri and Kroemer, 2001). Apoptosis leads programmed cell death carried out by the cell by cellular narrowing, membrane blabbing, chromatin condensation and nuclear fragmentation, followed by the formation of apoptotic bodies that are digested by phagocytic cells (Kerr et al., 1972).

On the other hand, autophagy is a regulated cellular process that eliminates damaged cytoplasmic organelles. It is a normal process that is involved in important functions such as cell growth, development, aging and immunity (Pallepati and Averill-Bates, 2012). Different stress conditions can increase the cell's autophagic activity as it is generally a path of adaptation to stress that promotes cell survival. Autophagy allows the formation of autophagosomes that incorporate the damaged cytoplasmic content (Lin and Baehrecke, 2015) subsequently its. Autophagosome membrane merges with lysosomes membrane forming an autolysosome where damaged organelles are degraded

by lysosomal enzymes such as cathepsins (Lin and Baehrecke, 2015). Autophagy is regulated by autophagy-related genes called *atg* and *mtor* (mammalian target of rapamycin) signaling pathway (Porta et al., 2011). In physiological conditions mTORC1 complex promotes cell growth and proliferation processes. When the cell is lacking in nutrients, mTORC1 is not more active, and another AMPK (AMP-activated protein kinase) complex, which senses nutrient deficiency (in particular ATP levels) activates the ULK kinase which autophosphorylates and which starts a cascade of phosphorylation including AMBRA1 and ATG14. Both AMBRA1 and ATG14 are part of the PI3KC3 complex (Phosphatidylinositol-3-Kinase ClassIII, Papinski and Kraft, 2016). That is responsible for phosphatidylinositol-3-phosphate (PI3P, Phosphatidyl Inositol 3 Phosphate) formation, a typical lipid of autophagosome membrane (Klionsky et al., 2016).

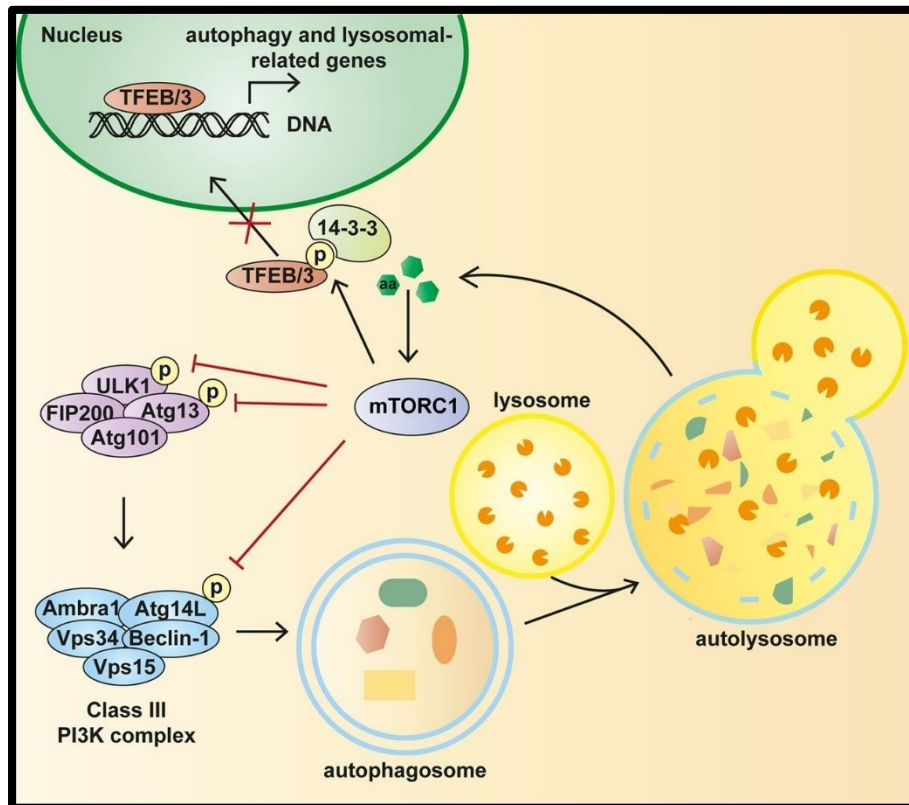


Fig.1.10 *mtor* and autophagy related gene signaling (Rabanal-Ruiz et al., 2017)

However, in stress conditions, the autophagic pathway can be activated independently from *mtor*. Several signaling cascades such as cAMP regulate autophagy independently of mTORC1 signaling. The increase in cAMP levels by adenylate cyclase (AC) activates a cascade of signals to generate inositol triphosphate (IP 3), which binds to its receptor present on the endoplasmic reticulum membrane allowing the release of Ca^{2+} ions stored in ER (Targos et al., 2005). Increase of Ca^{2+} ions in cytosol allows the activation of CALPAIN which inhibits autophagy. The PI3KC3 complex regulates autophagosome synthesis possibly downstream of mTOR-independent pathways, although the

mechanistic details remain clarified (Sarkar,2013). Autophagy, however, can also act as a pathway to cell death independent of caspases. Autophagic cell death is characterized by dying cells containing abundant autophagosomes, but the signaling pathways that regulate the process of autophagic death are still not entirely clear (Lin and Baehrecke, 2015).

1.3.2 Copper exposure induce inflammation and neuromast death in zebrafish larvae.

Incorporation and accumulation of copper in zebrafish larvae depend on the dose administered and the timing of exposure. (Leite et al., 2013); it has also been seen that the protein involved in copper metabolism in zebrafish (CTR1, ATOX1, ATP7A, ATP7B) compared with human ones have about 70% identity (Zhao et al., 2014). For this reason, Zebrafish is also an excellent experimental model for the study of copper metabolism and the associated diseases.

Mortality studies conducted on 3dpf zebrafish larvae found that concentrations above 25 μ M induced high mortality, while concentrations below 10 μ M showed mortality comparable to control (Hernández and Allende, 2008). D'Aleçon et al., 2010, conducted a study monitoring *in vivo* leukocyte migration following copper-induced damage. This study showed that exposure to 10 μ M CuSO₄ concentrations for 2h in larvae at 3dpf induce an oxidative

stress and oxidative damage followed by the destruction of neuromast of the lateral line. Oxidative damage and consequent destruction of the hair cells of the neuromast generated by copper sulphate induces an immune response through the migration of leukocytes around damaged neuromasts (D'Alecon et al., 2010). Neutrophils begin to migrate about 15 minutes after the start of exposure to copper sulfate and reach the damaged area within 20 minutes. The neutrophils remain in the damaged tissue for about 2-3 hours, after which they begin to disperse. Neutrophils are no longer detectable after 6 hours from the removal of copper sulfate (D'Alecon et al., 2010).

Hernandez et al. in 2011 conducted studies in which it was seen that after 35 minutes from the start to 10 μ M CuSO₄ exposure of zebrafish larvae at 72 hours post fertilization (72hpf), caused necrosis of hair cells and a partial damage of support cells of lateral line neuromast. Studies conducted on regeneration of lateral line hair cells have shown that the accessory neuromast cells exhibit upregulation of the *agt2bl*, a gene codifying for a factor involved in autophagy processes (Steiner et al., 2014), assuming that the autophagic process is involved in the regeneration of hair cells as occurs in the regeneration of the caudal fin where autophagy is necessary for regeneration (Varga et al., 2014). Furthermore, Zhang et al. in 2016 they showed that exposure to copper sulfate of zebrafish embryos in the early stages of development can cause a

postponement of hatching, problems in larval swimming and an inhibition of neurogenesis.

As we have seen, an excess of copper can cause oxidative damage which leads to the activation of different cellular processes aimed at repairing the damaged tissue and cell. We therefore decided to use zebrafish as a model organism to evaluate the beneficial properties of PD (discussed in section 1.2.2) by inducing oxidative stress by exposing zebrafish larvae to copper sulphate. Based on the mortality studies carried out by Hernandez et al., 2008, we decided to use $10\mu\text{M}$ $\text{CuSO}_4 \cdot 5\text{H}_2\text{O}$. PD concentrations were instead decided on the basis of studies conducted on zebrafish by Pardal et al., 2014. Although with different timing and objectives, they tested PD concentrations from $10\mu\text{M}$ to $2000\mu\text{M}$. Their results showed that with $100\mu\text{M}$ concentrations of PD there was a reduction in fatty acids at the yolk level. Based on these previous results we decided to check if an intermediate concentration ($400\mu\text{M}$) could have effects in the processes we wanted to study.

1.4 Genes analyzed

In section 1.3 was described that in zebrafish an excess of copper is responsible for oxidative damage that involves the activation of the immune system, antioxidant molecules and regenerative system in zebrafish lateral line.

In this regard, in the present study we wanted to analyze the expression of some genes involved in the repair of the damage suffered by the cell.

First, we wanted to analyze the genes involved in the immune system. Interleukins (IL) are a type of cytokines expressed by many cell types. IL allow the proliferation, maturation, migration and adhesion of immune cells. Cytokines are proteins that can be produced in response to pathogens or other factors that give rise to an inflammatory response of the damaged cell. Once expressed, cytokines are immediately secreted (Turner et al., 2014).

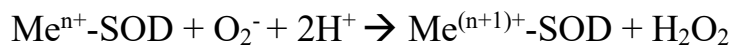
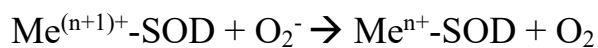
Interleukins mediate cellular up and down-regulatory responses by binding to specific cellular receptors. In fact, they may be responsible for activating other interleukins. (Vaillant et Qurie, 2019). In particular, we have analyzed:

- ❖ *il1*: IL-1 causes lymphocyte activation and stimulation of leukocyte cells. IL-1 is responsible for raising the body's basal temperature as it stimulates the release of acute phase proteins from the liver. It is also responsible for the activation of pro-apoptotic mechanisms in damaged cells (Boraschi and Tagliavue, 1996).
- ❖ *il8*: The main task of IL-8 is to recruit innate immune system cells such as neutrophils, basophils, mast cells and macrophages via chemotaxis (Hammond et al., 1995).

- ❖ *il10*: Interleukin 10 (IL-10) is an anti-inflammatory cytokine that regulates the production of pro-inflammatory molecules to limit tissue damage and maintain or restore tissue homeostasis (Mosser 2008).

Oxidative stress response was evaluated by analyzing the expression of genes with anti-oxidant activity. These are enzymes that suppress or prevent the formation of free radicals or reactive species in cells. We have analyzed:

- ❖ *sod1* and *sod2*: Superoxide dismutase (SOD) is an important endogenous antioxidant enzyme that allows a first-line defense against reactive oxygen species (ROS; Ighodaro and Akinloye, 2018). Based on protein folding and metallic cofactor that presents inside, Superoxide dismutase are divided in: SOD1(Cu/Zn-SOD), located in cytoplasm and SOD2 (Mn-SOD) located in mitochondria (Fridovich, 1995) and they catalyze follows reaction:



- ❖ *cat*: Catalase (CAT) is a tetramer with four similar subunits found in peroxisomes (Radi et al., 1993). CAT is an antioxidant enzyme that uses iron or manganese as a cofactor (Chelikani et al., 2004) and catalyzes the following reaction:



A damaged cell uses repair systems through the activation of autophagy or when the damage is not repairable by the activation apoptosis signals. Apoptosis is defined as programmed cell death (Type I cell death) and occurs through the activation of enzymes that lead to the rapid demolition of cellular structures and organelles. Autophagy allows parts of the cytoplasm and cytoplasmic organelles to be directed towards lysosomes for degradation. In many conditions, autophagy is a process of adaptation to stress that protects from cell death; at other times, however, autophagy becomes an alternative way of cell death, called "type II cell death" (Maiuri et al., 2007). In some circumstances, therefore, apoptosis and autophagy can exert synergistic effects, while in other situations autophagy can be induced only when apoptosis is suppressed (Amelio et al., 2011; Gonzalez-Polo et al., 2005). For this reason, we wanted to analyze the expression of the genes that regulate apoptosis and autophagy including:

- ❖ *mtor*: The mammalian target of rapamycin (mTOR, Sabers et al., 1995), is formed by two complexes: mTOR complex 1 (mTORC1) and mTOR complex 2 (mTORC2), which regulate different cellular processes (Kim et al., 2002). mTOR is a serine/threonine protein kinase and regulates cell growth, cell proliferation, cell motility, protein synthesis, autophagy and apoptosis (Hay et Sonenberg, 2004).

- ❖ *lc 3*: LC3 is a protein that in humans is encoded by the MAP1LC3B gene and is a protein involved in the process of autophagy and in particular in the formation of the membrane of the autophagosome (Klionsky et al., 2016). According to other studies, LC3 would be involved not so much in the biogenesis of autophagosomes, but above all in the fusion of the latter with lysosomes (Nguyen et al., 2016).
- ❖ *ambra1*: *ambra1* is a recently discovered gene and it is a crucial regulator of autophagy. Ambra1 interacts with Beclin which positively regulates the formation of autophagosomes (Fimia et al., 2013)
- ❖ *casp3*: Caspase-3 is a caspase encoded by the *casp3* gene. Caspase activation plays a central role in cellular apoptosis processes. Caspases are inactive proenzymes that undergo proteolytic shearing in aspartic residues to produce two subunits that dimerize and form the active enzyme (McIlwain et al., 2013).
- ❖ *p53*: tumor protein 53, is a transcription factor that regulates the cell cycle and acts as a tumor suppressor. In cells damaged, if DNA damage is irreparable, p53 can initiate apoptosis, inducing transcription of *noxa*, if the DNA is repaired, p53 is degraded and the cell cycle is resumed (Finlay et al., 1989).

In zebrafish larvae, copper sulfate exposure induces lateral line hair cell death. In paragraph 1.1.4 we described that these cells have the ability to regenerate. For this reason, we analyzed genes expression involved in regenerative processes of zebrafish lateral line including:

- ❖ *cldn b*: Claudins are a family of proteins that, along with occludin, are the most important components of tight junctions. *claudin b* is expressed at high levels in the neuromast supporting cells of the lateral line and is involved in the development of neuromasts and motor neurons (Sonnack et al., 2018).
- ❖ *phoenix*: phoenix is a protein expressed in neuromast support cells. As we saw in paragraph 1.1.4 its function is not yet known, but it seems to be involved in the regeneration processes of the lateral line.

We also evaluated some genes involved in cell proliferation:

- ❖ *cyclin B* and *ccna 2*: Cyclins are proteins that regulate the cell cycle associated with the enzyme cyclin-dependent kinase (CDK). Their concentration varies during the cell cycle. At low concentrations the cyclins tend to dissociate from the CDK and assume an 'inactive' conformation. Cyclins have binding sites for some substrates and direct

CDKs to specific cellular locations (Crosby, 2007). There are four classes of cyclins:

- The G1 cyclins are transcribed during G1 phase of the cell cycle and they are constituted by cyclins D. Their function is to control G1/S cyclins activity.
- The G1/S cyclins are widely transcribed in the late G1 phase and are represented by the family of cyclins E. As soon as the cell enters phase S, the levels of this cyclin collapse.
- The S cyclins are represented by cyclins A family, transcribed by *ccna2* gene. These are already transcribed in the late G1 phase but reach the maximum concentration in S phase and persist until the transition from metaphase to anaphase phase of mitosis cycle, after which the levels collapse sharply. These cyclins stimulate the duplication of DNA and participate in the regulation of the first phases of mitosis.

The G2/M cyclins, transcribed by *cyclin B* gene at beginning of the G2 phase up to anaphase of mitosis process, after which they collapse in favor of the G1 cyclins. In particular, cyclin B is also called "mitotic cyclin ". The CDK

and Cyclin B complex is called mitosis promoting factor (MPF) which is a factor that promotes mitosis.

2. RESEARCH OBJECTIVE

Numerous studies have shown the different beneficial properties of PD (Şöhretoğlu et al., 2018; He et al., 2012; Ban et al., 2010; Zhao et al., 2010; Zhang et al., 2006; Huang et al., 1999; Ji et al., 2012) in particular, have been studied its antioxidant (Wang et al. 2015) and anti-inflammatory (Ravagnan et al., 2013) properties.

The objective of this study was to evaluate PD beneficial properties in the zebrafish larvae development in which an oxidative stress was induced by exposing zebrafish larvae to CuSO₄ (Pereira et al., 2015).

In particular, we wanted to evaluate whether PD was more effective as a preventive antioxidant and anti-inflammatory substance, administering it before CuSO₄, or if it was more effective as a curative substance, administering it after copper exposure.

In zebrafish larvae, copper sulfate exposure also causes the lateral line hair cells death (Hernandez et al., 2007), which can regenerate itself. For this reason, we wanted to assess whether PD administered before copper exposure reduce neuromasts death and if it allowed a more rapid regeneration of the hair cells.

3. MATERIALS AND METHODS

3.1 Tanks set up, coupling, collecting and maintaining embryos

Zebrafish larvae used in this work were obtained from adult zebrafish bred in the Department of Life and Environmental sciences, at Polytechnic University of Marche.

About 30 male and female specimens of zebrafish are bred in 100-liter tanks equipped with mechanical and biological filters, in which water temperature was regulated around 25° C with the use of thermostats. Was imposed an optimal photoperiod of 13 hours of light and 11 hours of darkness, obtained thanks to lamps equipped with timers that turn on at 6:00 and go out at 19:00. Adult zebrafish are fed twice a day with *Artemia nauplii*, frozen adult artemia (Eschematteo - Parma, Italy) and dry granular food enriched with Algamac 3050 (PTAqua - Sandyford, Dublin, Ireland) an enrichener of fatty acid.

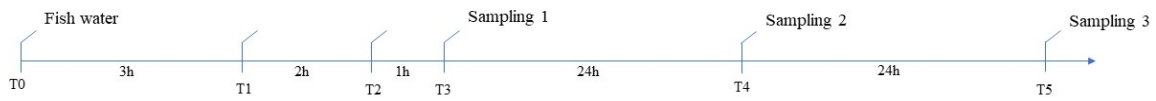
Evening before coupling, about 10 males and 10 females were transferred in tanks with a double bottom. Mating occurs at the first light of dawn. Females release the eggs and males release spermatozoa, with consequent fertilization. Embryos fall to the bottom and are separated from the parents by a net that acts as a filter, this prevents adults eating embryos. To increase the hatching yield

and decrease the number of moldy embryos, in the morning tank water was filtered by a net and the embryos were collected and transferred to a 20l cylindrical hatch equipped with ventilation and filled with the same water as the original tank. After 24 hours, embryos were counted at the stereomicroscope (Leica Wild M3B, Leica Microsystem - Buccinasco (MI), Italy), subsequently they were transferred into small trays with E3 medium (5mM NaCl; 0,17mM KCl; 0,33 CaCl₂; 0,3 mM MgSO₄; pH=7) and kept at 28.5 ° C until hatching.

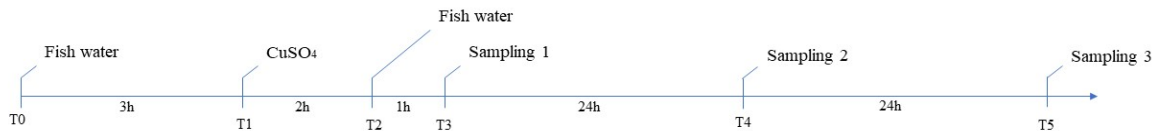
3.2 Experimental design

1080 embryos were divided equally into 18 trays (3 trays for each experimental group). Embryos were maintained in E3 medium, commonly called Fish Water, at a temperature of 28.5°C up to hatching (T0, 72 hpf) so we proceeded with the experimentation as shown in Figure 3.1.

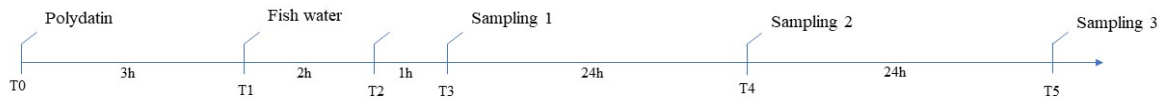
CTRL Group



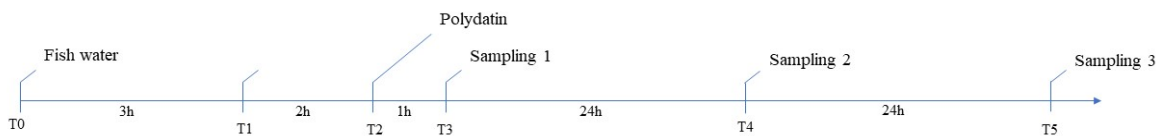
CuSO₄ Group



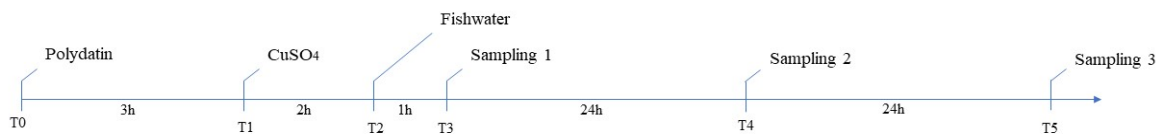
PD - T0 Group



PD - T2 Group



PD - T0 + CuSO₄ - T1 Group



CuSO₄ - T1 + PD - T2 Group

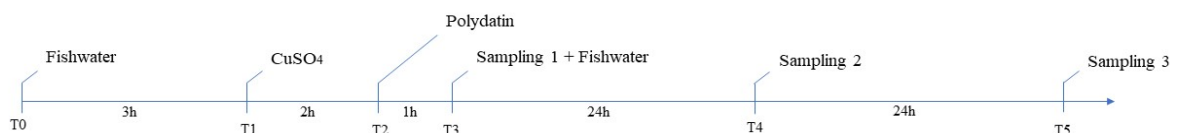


Fig.3.1 Experimental design with copper exposure. The abbreviations as in text mean PD=polydatin, T0=72hpf, T1=75hpf, T2=77hpf, T3=78hpf, T4=102hpf, T5=126hpf.

Experiment included 6 experimental groups:

- 1) Control (CTRL group): control group larvae were kept in fish water for all experiment.
- 2) $\text{CuSO}_4 \cdot 5\text{H}_2\text{O}$ (CuSO_4 group): larvae at T1 (75hpf) were immersed in a solution containing $10\mu\text{M}$ $\text{CuSO}_4 \cdot 5\text{H}_2\text{O}$ for 2h. After copper sulfate exposure larvae were transferred back to the fish water until the end of the experiment.
- 3) Polydatin 72hpf (PD-T0 group): larvae at T0 (72hpf) were immersed in a $400\mu\text{M}$ polydatin solution for 3 hours, subsequently (T1 – 75hpf) they were transferred back to the fish water until the end of the experiment.
- 4) Polydatin 77hpf (PD-T2 group): larvae were kept in fish water until T2 (77hpf) time. At this point they were immersed in a solution of $400\mu\text{M}$ PD for 1 hour and then transferred back to fish water (T3-78hpf).
- 5) Polydatin 72hpf + CuSO_4 75hpf (PD-T0+ CuSO_4 -T1 group): larvae at T0 (72hpf) were immersed in $400\mu\text{M}$ Polydatin for 3 hours, after which they were exposed to $10\mu\text{M}$ $\text{CuSO}_4 \cdot 5\text{H}_2\text{O}$ for 2 hours (T1-75hpf). They were later transferred to fish water(T2-77hpf).
- 6) CuSO_4 75hpf + Polydatin 77hpf (CuSO_4 -T1+PD-T2 group): larvae were kept in fish water until T1(75hpf) time. At this point larvae were exposed to $10\mu\text{M}$ $\text{CuSO}_4 \cdot 5\text{H}_2\text{O}$ for 2 hours. Subsequently larvae were transferred

in 400 μ M Polydatin for 1 hour (T2-77hpf) and then transferred back to fish water (T3-78hpf).

In results and in discussion, the groups 5 and 6 will be indicated with CuSO₄+PD and PD+CuSO₄ respectively.

The solutions were obtained by dissolving 10 μ M CuSO₄·5H₂O (PM=249,677 g/mol; Sigma Aldrich - Darmstadt, Germany) and Polydatin (PM 390,38g/mol; Sigma Aldrich - Darmstadt, Germany) in E3 medium at room temperature.

For the study of inflammation, in addition to copper sulphate exposure, we performed an incision in the caudal fin. 45 embryos were separated into 9 trays (3 for each experimental group) and kept in fish water up to T0 (72hpf).

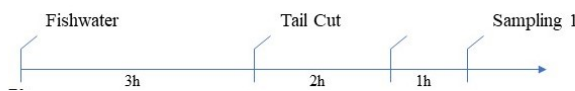
In T0 (72hpf) we performed the experiment that included 3 experimental groups:

- 1) Tail cut group: larvae were kept in fish water up to T1(75hpf). At this point the larvae suffered an incision of the of the caudal fin near the end of the blood flow, since in the larvae at this stage the caudal fin does not yet develop the bifurcation and were transferred back to the fish water.
- 2) Polydatin 72hpf + Tail cut (PD-T0+Tail cut group): At T0(72hpf) time larvae were transferred in 400 μ M PD solution for 3 hours. At T1(75hpf) larvae were subjected to the caudal fin incision and transferred back to the fish water until the end of the experiment.

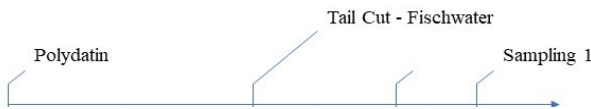
3) Tail cut + Polydatin 77hpf (Tail cut+PD-T2 group): larvae were kept in fish water up to T1(75hpf). At this point the larvae suffered an incision of the caudal fin and were transferred back to the fish water. At T2(77hpf) time larvae were transferred in in 400 μ M Polydatin solution for 1 hour.

For this experiment larvae were all sampled at T3(78hpf) time.

Tail Cut Group



PD - T0 + Tail Cut Group



Tail Cut + PD - T2 Group

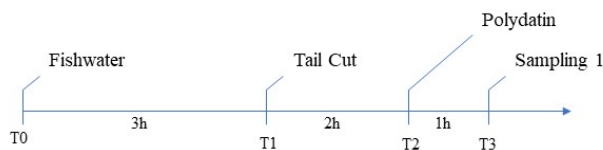


Fig.3.2 Experimental design with cut tail. The abbreviations as in text mean PD=polydatin, T0=72hpf, T1=75hpf, T2=77hpf, T3=78hpf.

Larvae subjected to caudal fin incision were anesthetized in 15mg/ml MS-222 solution (Tricaine methanesulfonate, TMS, Sigma Aldrich - Darmstadt, Germany). The incision was made to the stereomicroscope with a scalpel.

3.3 Morphological analysis

For morphological analyzes larvae were photographed with Microscope Camera (DeltaPix - Smorum, Denmark) at the stereomicroscope (Optech Microscope Services Limited -Thame, Oxfordshire).

For all morphological analysis a total number of 10 larvae were analyzed for each experimental group.

3.3.1 Length measurement

Fish length was measured from the end of the head to the end of the tail, excluding the caudal fin. The measures have been related to the respective ones scale bar measurements, to obtain data expressed in μm . The length was measured in larvae sampled at T4 and 5 sampling at T5 to evaluate differences in growth between various experimental groups during development.

3.3.2 Swim bladder development and dorsal curvature

To evaluate alterations of embryonic development, we observed 2 parameters in larvae sampling at T5: swim bladder insufflation and larva dorsal curvature.

We counted the number of larvae showing correct swim bladder development and the number of larvae with a dorsal curvature (scoliosis). These data were reported as larvae percentage.

3.4 Myeloperoxidase (MPO) test

We used the myeloperoxidase test for an inflammation rapidly screen. This test is a cytochemical staining system for the detection of polymorphonuclear leukocytes, in particular of neutrophils. Myeloperoxidase test allowed us to perform a qualitative analysis of neutrophil migration in sites damaged by exposure to copper sulfate and the caudal fin incision. Being a rapid test, we used it primarily to optimize the sampling times after copper exposure and subsequently based on these results, we performed a different test to optimize the best timing for polydatin treatment. This test uses diaminobenzidine (DAB; Sigma Aldrich - Darmstadt, Germany) as a dye, which reacts with H_2O_2 and it colors cell in brown. The reaction is catalyzed by myeloperoxidase, an enzyme produced by neutrophils, able to promote an inflammatory response.

After T3 sampling larvae were set overnight in 4% paraformaldehyde (PFA). After fixation, 3 washes with PBS 1X (Phosphate buffered saline) were performed for 10 minutes. Subsequently Incubation Mix was prepared as

follows: TRIS was first prepared by dissolving 2,42g of Trisma Base in 100ml of H₂O deionized. Work solution was then prepared using 100ml of TRIS and 1ml of HCl. 12,5 mg of DAB were dissolved in 25 ml of work solution and 37,5 µl of H₂O₂ were added shortly before immersing the larvae in the solution. Larvae remain in work solution for about 5-10 minutes, once the larvae coloration has been verified under the microscope, the reaction was blocked in deionized H₂O. Results were detected at Zeiss microscope (Axio Imager 2) with combined Axiocam 506 monochrome camera. For all MPO test analysis a total number of 10 larvae were analyzed for each experimental group.

For all MPO tests a total number of 10 larvae were analyzed for each experimental group.

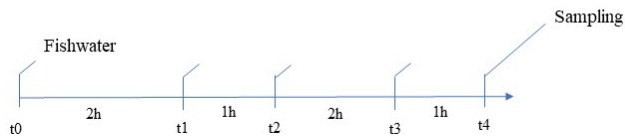
3.4.1 Sampling time test after copper sulfate exposure

To assess what was the best sampling times to evaluating neutrophil migration we performed a preliminary test. The test involved exposing larvae sampling at 3dpf to 10µM CuSO₄·5H₂O for 2 hours, then larvae were transferred in Fish Water. We did 3 sampling, respectively 1h, 3h and 6h after the end of copper sulphate exposure. Sampled larvae were fixed in 4% PFA for myeloperoxidase test.

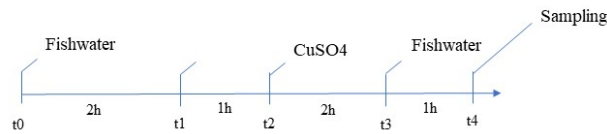
3.4.2 Polydatin treatment timing test

To evaluate the best treatment times with polydatin we performed a test based on the previous test. To carry out this test, we divided 60 embryos into 4 trays (one for each experimental group) containing fish water. The experiment starts at 72hpf and was performed as in Figure 3.4.1.

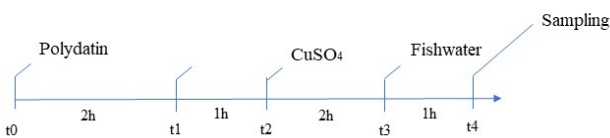
CTRL Group



CuSO₄ Group



PD + CuSO₄-t₂ Group



PD - t₁ + CuSO₄-t₂ Group

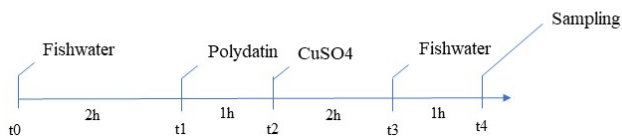


Fig.3.3 Experimental design polydatin timing test. The abbreviations as in text mean PD=polydatin, t₀=72hpf, t₁=74hpf, t₂=75hpf, t₃=77hpf, t₄=78hpf. t (small format) indicates the timing for polydatin treatment timing test.

The timing test of polydatin treatment timing is indicated with t (small letter) to distinguish them from the times used in the previous experiment indicated with T (uppercase letter).

- 1) Control group (CTRL group): larvae were kept in fish water for all experiment.
- 2) $\text{CuSO}_4 \cdot 5\text{H}_2\text{O}$ (CuSO_4 group): at $t_2(75\text{hpf})$ larvae were exposed to $10\mu\text{M}$ $\text{CuSO}_4 \cdot 5\text{H}_2\text{O}$ for 2 hours and then were transferred back to the fish water for 1h ($t_3-77\text{hpf}$).
- 3) Polydatin $72\text{hpf} + \text{CuSO}_4$ 75hpf (PD- $t_0 + \text{CuSO}_4 - t_2$): larvae at t_0 (72hpf) were immersed in $400\mu\text{M}$ Polydatin for 3 hours, after which they were exposed to $10\mu\text{M}$ $\text{CuSO}_4 \cdot 5\text{H}_2\text{O}$ for 2 hours ($t_2-75\text{hpf}$). They were later transferred to fish water($t_3-77\text{hpf}$).
- 4) Polydatin $74\text{hpf} + \text{CuSO}_4$ 75hpf (PD- $t_1 + \text{CuSO}_4 - t_2$): larvae were kept in fish water up to t_1 (74hpf). At this point larvae were immersed in $400\mu\text{M}$ Polydatin for 1 hour, after which they were exposed to $10\mu\text{M}$ $\text{CuSO}_4 \cdot 5\text{H}_2\text{O}$ for 2 hours ($t_2-75\text{hpf}$). They were later transferred to fish water($t_3-77\text{hpf}$).

All larvae were sampled at $t_4(78\text{hpf})$ and fixed in 4% PFA for myeloperoxidase test.

3.5 DASPEI staining

To evaluate the intactness of lateral line cells, we performed an *in vivo* staining with DASPEI (2- (4- (dimethylamino) styryl) -N-Ethylpyridinium Iodide) that labels hair cell mitochondria. To obtain a concentration of 1mM, 0.19g of DASPEI (PM = 380.77 Invitrogen - Loughborough, Leicestershire) in 50 ml of E3 medium were dissolved. At T3 ten larvae for experimental group were immersed in the DASPEI solution for 5 minutes, rinsed in E3 medium, killed in a lethal dose (30mg/ml) of MS222 and observed with Zeiss epifluorescence microscope (Axio Imager 2 – Berlin, Germany) with combined AxioCam 506 monochrome camera. The fluorescence emission spectrum was set at 450 nm and the filter used for the acquisition was set at 515nm. The images acquired in black and white were then processed using ZEN2.3 software in order to attribute green color at the fluorescence and eliminate unspecific background. For DASPEI staining a total number of 10 larvae were analyzed for each experimental group.

The first neuromast of the posterior lateral line (L1) was chosen to evaluate lateral line regeneration. After 24h (T4) other 10 larvae from each experimental group were stained and observed again to evaluate the regeneration of the L1 neuromast.

3.6 Semi-quantitative Real-time PCR (RT-PCR) analysis.

3.6.1 Sampling

For RT-PCR analysis larvae were sampled at T3 and for each experimental group we taken 6 replicates with 30 larvae each one. Larvae were transferred in 1.5ml dry Eppendorf and placed on dry ice for transport and stored in laboratory freezers set at -80 °C till their analysis.

3.6.2 RNA extraction

For RNA extraction from each sample we used the following protocol:

- the sample stored in freezers set at -80°C was quickly thawed at room temperature
- 800µl of RNAzol (Sigma Aldrich - Darmstadt, Germany) were added to the sample
- The mix (sample+RNAzol) was transferred to a clean glass cuvette using a glass pasteur
- the sample was homogenized for 10 seconds at medium speed with homogenizer with pestle in teflon (T 25 digital ULTRA-TURRAX® - IKA – Staufen, Germany)

- the homogenate was transferred in a new 1,5ml eppendorf and diluted with 320 μ l autoclaved water
- the solution was vortexed for 15 seconds and then left at room temperature for 15 minutes
- subsequently the solution was subjected to a centrifugation of 12000g for 15 minutes at 4 ° C
- after centrifugation RNA is in the supernatant that is taken and transferred to a new eppendorf
- based on the amount of supernatant taken, the same amount of isopropanol was added
- supernatant+isopropanol was left in at room temperature for 10 minutes and then subjected to a centrifugation of 10,000 g again for 10 minutes at 4 ° C
- After centrifugation, RNA precipitates in a pellet, the supernatant was removed and 400 μ l of 75% ethanol were added
- a centrifugation of 10000g was carried out for 5 minutes at 4 ° C.
- the last 2 step steps are repeated 2 times

- after second centrifuge, the supernatant was removed to be ensure that all ethanol was removed and the sample was left for 2-3 minutes in chemical hood with the eppendorf cap open
- finally, pellet was diluted in 10 μ l of autoclaved water.

Whole process must be carried out under a chemical hood because RNazol and isopropanol reagent are very toxic.

RNA concentration (μ g/ μ l), the ratio 260/280 (protein contamination index) and the ratio 260/230 (phenol contamination index) were measured by NanoPhotmeter P-Class (Implen - München, Germany).

RNA was stored in freezers set at -80°C.

3.6.3 Electrophoresis gel

RNA quality was determined by electrophoretic run on 1% agarose gel. For gel preparation, 1g of agarose was dissolved in 100 ml of solution consisting of 98ml of deionized water and 2ml of TAE 50X. The solution was up to 150 °C on heater and mixed using a magnet until boiling.

After removing the solution from the plate, it was left at room temperature for a few minutes and when the solution has reached a warm temperature, 6 μ l of Midori Green Advance have been added (NIPPON Genetics Europe – Dueren,

Germany). Everything was poured into the mold with a special tool for forming the wells and left to cool. The gel can be stored in the fridge at 4°C for a few days.

For the electrophoretic run, an eppendorf number equal to samples number was prepared. In each Eppendorf was added 9µl of autoclaved water, 2µl of TAE blue and 1µl of RNA thawed at room temperature (for a final volume of 12µl).

Gel is placed in a tray and submerged by the TAE1X and the solution was placed in the gel wells. The tank is connected to electrodes and generator was set to 120Volt. After a run of about 20 minutes RNA migrated to the positive pole with the separation of 28S,18S and 5S ribosomal RNA bands.

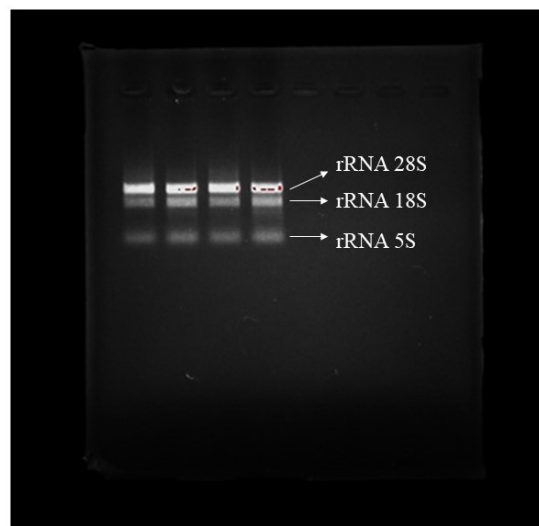


Fig.3.4 Electrophoresis run of 4 samples (2 from control group and 2 from CuSO₄ group).

3.6.4 DNase treatment

Enzymatic digestion with DNase has been performed to clean RNA sample from any DNA contamination. For DNA treatment it was used DNase I (Sigma Aldrich - Darmstadt, Germany) kit. 4µg of RNA dissolved in 8µl of autoclaved water were transferred into 1.5ml eppendorf. In each eppendorf, 1µl of 10X Reaction Buffer and 1µl of DNase were added to allow DNA degradation. Samples were incubated for 15 minutes at room temperature. Subsequently in each sample it was added 1µl of stop solution to bind calcium and magnesium and block DNase activity. Samples are finally placed in the thermocycler (MyCycler Thermal Cycler System - BioRad - California, USA) for 10 minutes at 70°C. After treatment with DNase, for each sample it was re-measured RNA concentration and the ratios 260/280 and 260/230. The process was performed under the laminar flow hood trying to keep the RNA at room temperature as little as possible to avoid its degradation.

3.6.5 Reverse transcription

To obtain the cDNA it was used High-Capacity cDNA Reverse Transcription kit (Applied Biosystem - Carlsbad, CA, USA).

For each sample 2µg of RNA, diluted in 10µl of autoclaved water, were transferred in minieppendorf, and were added in sequence 2µl of RT Buffer

10X, 0.8µl of dNTPmix 25X, 2µl of Random Primers 10X, 1µl of Multiscribe RT and 4.2µl of autoclaved water for a final volume of 20µl. Miniependorfs were established in thermocycler (MyCycler Thermal Cycler System - BioRad - California, USA) by setting the kit protocol which includes 10 minutes at 25°C, 120 minutes at 37°C, 5 minutes at 85°C and the last step at 4°C that marks the process end. cDNA concentrations, and ratios 260/280 and 260/230 were measured on nanodrop (NanoPhotmeter P-Class, Implen - München, Germany). The process was performed under the laminar flow hood trying to keep the RNA at room temperature as little as possible to avoid its degradation.

3.6.6 Semi-quantitative RT-PCR

To assess gene expression, it was performed semi-quantitative Real Time -PCR (RT-PCR). RT-PCR includes a first step in which there is the preparation of a 96-well plate and is carried out under a laminar flow hood to avoid any type of contamination. In each well 1µl of cDNA, with a 1:10 dilution, and 9µl of MIX were inserted. The MIX for each sample contains 5µl of Syber Green (Fluocycle II SYBER Master MIX - Euroclone SpA - Pero (MI), Italy), 3.8µl of autoclaved water and 0.2µl of forward and 0.2µl reverse primers. Each sample was prepared in duplicate. Subsequently the plate was placed in iQ5 iCycler thermocycler (CFX Connect Real-Time PCR Detection System- Hercules, CA, USA) and it was applied a specific protocol for each analyzed

gene. The general protocol includes: 3 minutes at 95°C followed by 45 cycles of 20 seconds at 95°C (denaturation), 20 seconds at T melting depending on the primer used (annealing) and 20 seconds at 72°C (elongation). At the end of each cycle the emission of fluorescence was monitored. The housekeeping genes used were *arp* and *rpl 13*. The primers used are shown in Table 1 below. Results were analyzed using the IQ5 optical system V 2.0 software which includes Genex Macro iQ5 Conversion and Genex Macro iQ5 files.

Gene	Primer Forward	Primer Reverse	Tm (°C)
<i>il 1</i>	GTGGATTGGGGTTTGATGTG	GCTGGGGATGTGGACTTC	54°C
<i>il 8</i>	ACTCGGACTGAAGGTGACTC	CCACGTCTCGGTAGGATTGAG	58°C
<i>il 10</i>	GCTCATTGTGGAGGGCTTTC	ATTGGGGTTGTGGAGTGCTT	56°C
<i>sod 1</i>	GTCGTCTGGCTTGTGGAGTG	TGTCAGCGGGCTAGTGCTT	60°C
<i>sod 2</i>	CCGGACTATGTTAAGGCCATCT	ACACTCGGTTGCTCTCTTTTCTCT	60°C
<i>cat</i>	CCAAGGTCTGGTCCCATAAA	GCACATGGGTCCATCTCTC	60°C
<i>mtor</i>	AACCTACTGCCTCGACTTGC	CTCACAGCCACCACCAGTAG	60°C
<i>ambra 1</i>	TCTTTCGAGAAATGGCACCT	CTCTCTGCGTTAGGGACAGG	60°C
<i>lc 3</i>	GAGAAGTTTTTGCCGCTCT	ACCTGTGTCCGAACATCTCC	60°C
<i>casp 3</i>	GTGCCAGTCAACAAACAAAG	CATCTCCAACCGCTTAAAG	60°C
<i>p53</i>	GGCTCTTGCTGGGACATCAT	TGGATGGCTGAGGCTGTTCT	60°C
<i>cldn b</i>	GAAGGAATTTGGATGAGCTGCGTGG	CGACAGCATGATTCCCATCAGTCG	56°C
<i>phoenix</i>	AAGTGAAGTCCCCACAAGTCC	TCACCATCTGACCAACATCCC	52°C
<i>cyclin b</i>	ATTCGGCCGAGGAGAATAGT	GAGCCATCATTCTCGTGGT	57°C
<i>ccna 2</i>	AAGCAGCTAACAAACAGGACAG	GTGGATCTCTGTAAAGGTGC	58°C
<i>arp</i>	CTGAACATCTCGCCCTTCTC	TAGCCGATCTGCAGACACAC	60°C
<i>rpl 13</i>	TCTGGAGGACTGTAAGAGGTATGC	AGACGCACAATCTTGAGAGCAG	59°C

Table 3.1 The table shows forward and reverse primers sequences and primer Melting Temperature (Tm) for each analyzed gene.

3.7 Statistic analysis

For statistical analysis it was used GraphPad Prism 6 Software. The type of analysis used was One-way ANOVA non-parametric. Data were transformed when necessary to meet the homogeneity of variance and normal distribution. The significance was set at $p < 0.05$.

4. RESULTS

4.1 Morphological analysis

Fig.4.1 shows how the length and morphology parameters have been taken, the images shown are representative of each single experimental group, the white arrow is used to indicate the spinal cord dorsal curvature and the black one to indicate the swim bladder. The respective results of length, curvature and bladder are discussed in the following paragraphs 4.1.1 and 4.1.2.

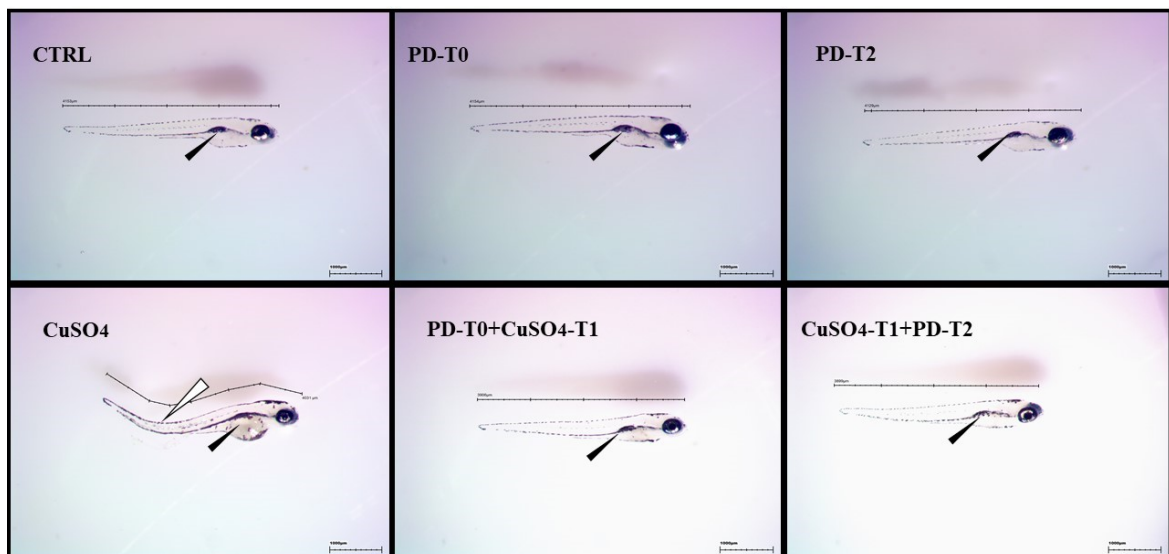


Fig.4.1 Representative picture of zebrafish larvae, sampling at T5, exposed to copper sulphate and polydatin treatments (Scale 1000 μ m). Black arrows indicate the presence of the swim bladder while white arrow spinal cord curvature.

4.1.1 Length measurement

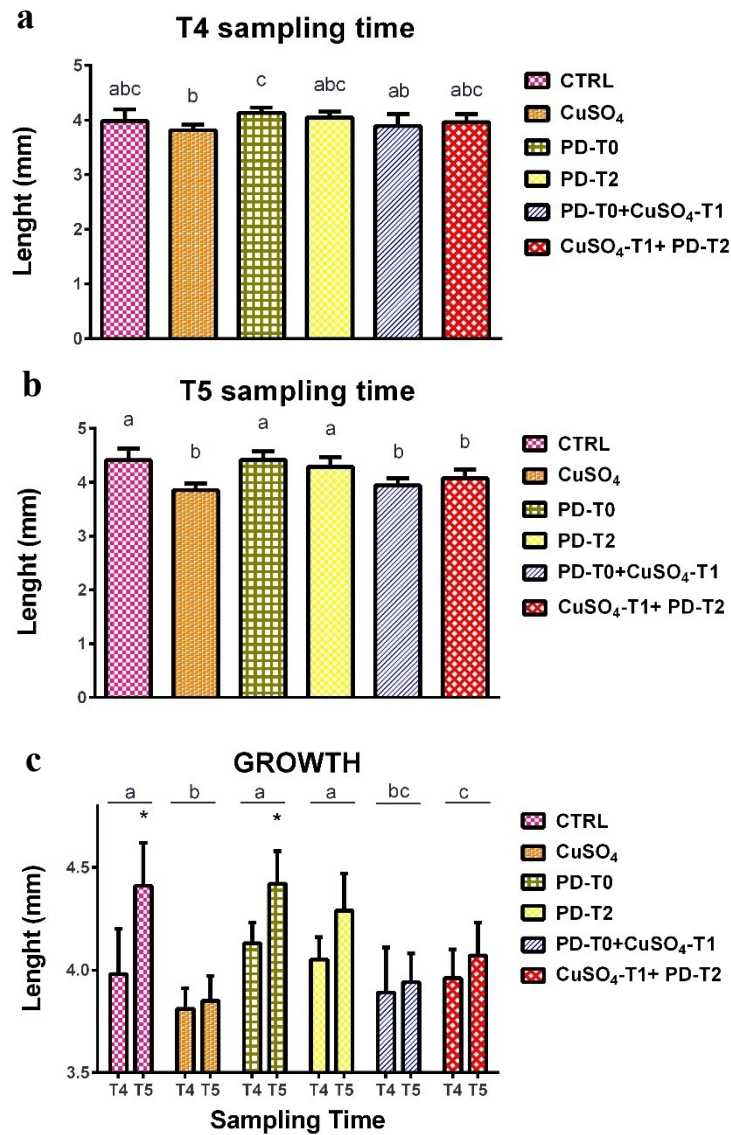


Fig.4.2 Figure show the lengths (mm) of larvae sampled at T4 (a) and T5 (b), letters indicate significant differences ($p < 0.05$) and the growth in length of the larvae between T4 and T5 sampling time (c). In c asterisks indicate significant differences in length between larvae sampled at T4 and larvae sampled at T5, while letters indicate differences in larvae growth between various experimental groups ($p < 0.05$).

Figure 4.2, panel a, shows the length (mm) of larvae sampled at T4 time. We found that there are significant differences only between larvae of PD-T0 group and larvae exposed to CuSO_4 after treatment with polydatin, and between larvae treated only with copper sulphate and PD-T0 group.

Figure 4.2, panel b, shows the differences between the lengths (mm) of larvae sampled at time T5. Also, here, there are not significant differences between the lengths of the control, PD-T0 and PD-T2 groups. Lengths of larvae belonging to CuSO_4 , PD+ CuSO_4 and CuSO_4 +PD groups are not significantly different from each other, but have a significantly lower length than control, PD-T0 and PD-T2 groups.

Figure 4.2, panel c, shows the length difference in the same experimental groups between larvae sampled at T4 and larvae sampled at T5, this significance is indicated with asterisks (*). These differences have also allowed us to calculate larvae growth difference between various experimental groups, the significant differences were indicated with letters. From the Figure 4.2 it can be inferred that control and PD-T0 are only groups that showed a significant growth between T4 and T5. On the other hand, there are not differences in growth between control, PD-T0 and PD-T2 groups. The growth of CuSO_4 group is significantly lower than the growth of control, PD-T0 and PD-T2 groups. As for CuSO_4 group the growth of larvae of CuSO_4 +PD group is

significantly lower than groups not treated with CuSO_4 , but significantly higher than CuSO_4 group. The growth of larvae of PD+ CuSO_4 group does not present significant differences respect to the CuSO_4 and CuSO_4 +PD groups, but it is significantly lower than control, PD-T0 and PD-T2 groups.

4.1.2 Swim bladder development and dorsal curvature

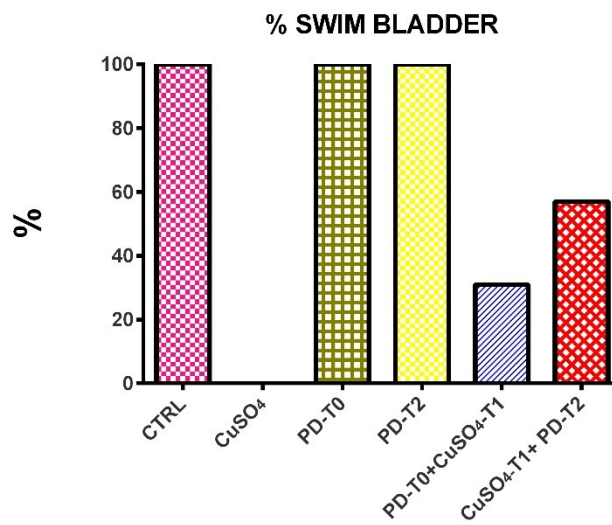


Fig. 4.3 The figure shows the percentage of larvae with correct swim bladder insufflation at T5.

The Figure 4.3 shows that all control group larvae and all larvae treated with polydatin alone (PD-T0 and PD-T2) have insufflated swim bladder (100%). None of the larvae exposed to $10\mu\text{M}$ $\text{CuSO}_4 \cdot 5\text{H}_2\text{O}$ has a correct swim bladder development (0%). Only 31% of larvae treated with polydatin before copper sulphate exposure (PD+ CuSO_4) have insufflated swim bladder, while the 57%

of larvae, first exposed to copper sulphate and then treated with polydatin (CuSO_4+PD), show a correct swim bladder development.

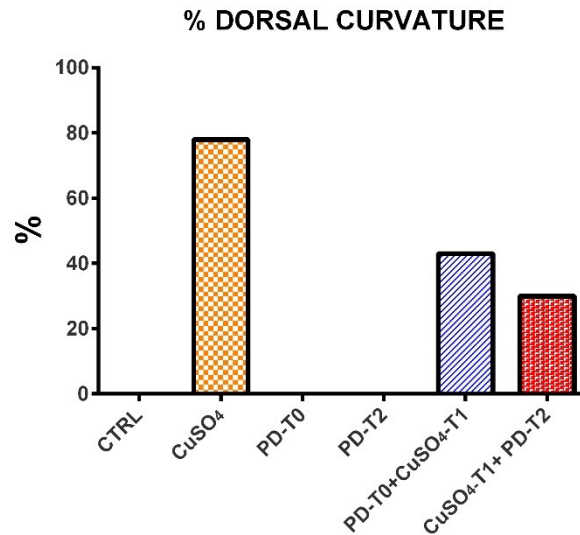


Fig.4.4 The graph shows the percentage of larvae with a dorsal curvature at T5.

Figure 4.4 shows the percentages of larvae that had a dorsal curvature after copper sulfate treatment. Larvae of control group and PD-T0 and PD-T2 groups don't show morphological alterations, while 78% of larvae exposed to $10\mu\text{M}$ $\text{CuSO}_4\cdot 5\text{H}_2\text{O}$ had a dorsal curvature. Polydatin treatments before and after copper exposure reduce the percentage of larvae showing a dorsal curvature. In fact, only 43% of PD + CuSO_4 group larvae had a dorsal curvature, and only 30% of CuSO_4+PD group larvae had a dorsal curvature.

4.2 MPO TEST

4.2.1 Sampling time test after copper sulfate exposure

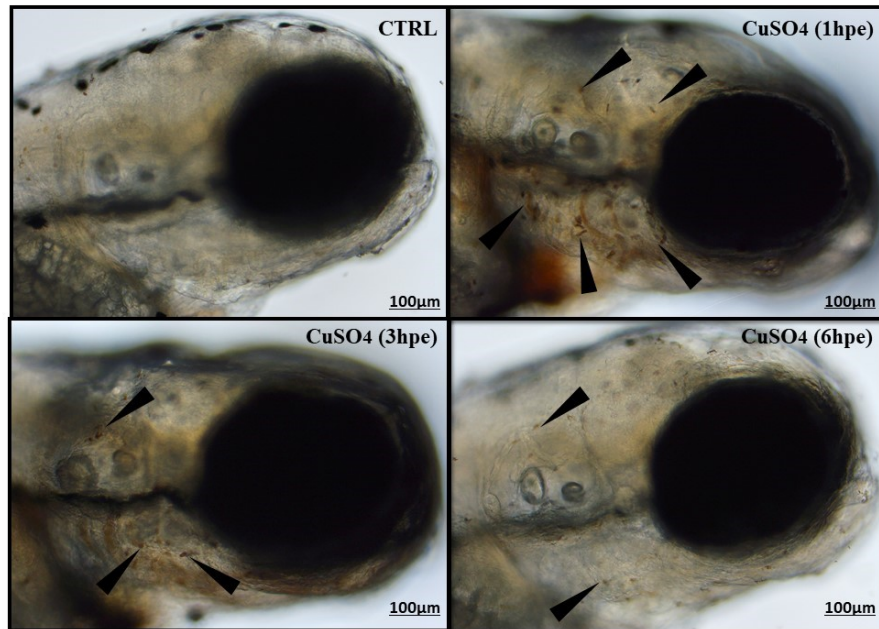


Fig.4.5 Figure shows representative images of neutrophils presence in the head of the control group larvae (CTRL) and larvae treated with copper sulphate and sampled respectively: one hour after the exposure end (CuSO₄ 1hpe), 3 hours from exposure end (CuSO₄ 3hpe) and 6 hours after exposure end (CuSO₄ 6hpe). Black arrows indicate neutrophils. Scale 100µm.

Figure 4.5 shows that in the head of the control group larvae no neutrophils are evident, by contrast to the larvae sampled one hour after copper sulfate treatment end (CuSO₄ 1hpe) that show a massive migration of neutrophils. A clear trend of decrease over time of neutrophils migration from 1 hour to 6

hours after CuSO_4 exposition. At 6 hrs, sampling situation was similar to the control.

4.2.2 Polydatin treatment timing test

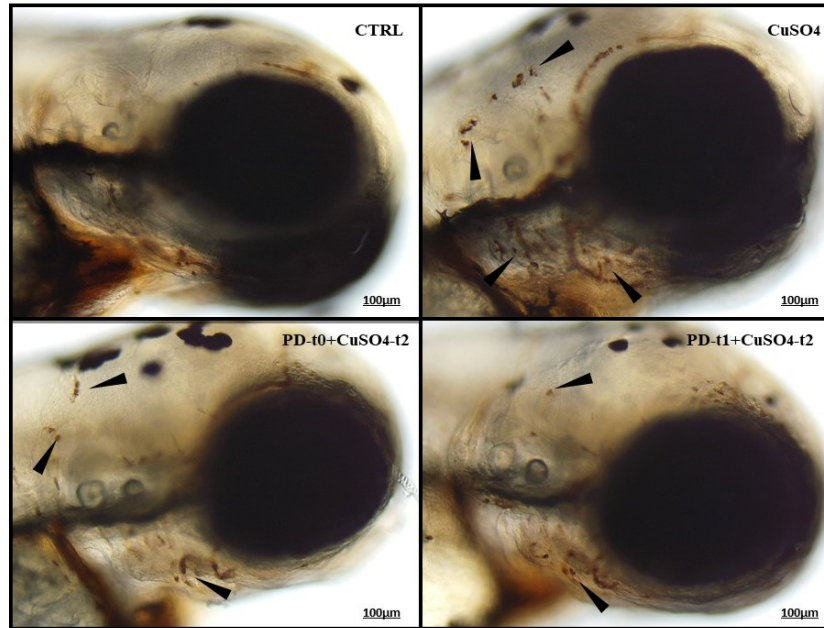


Fig. 4.6.a. The figure shows representative images of neutrophil migration in the head of the larvae. Photos represent the four experimental groups: control group larvae (CTRL), larvae treated only with copper sulfate (CuSO_4), larvae treated with polydatin for 3 hours before copper exposure (PD-t0 + CuSO_4 -t2) and larvae treated with polydatin for 1 hour before copper exposure (PD-t1+ CuSO_4 -t2). Neutrophils are indicated with black arrows. Scale 100µm.

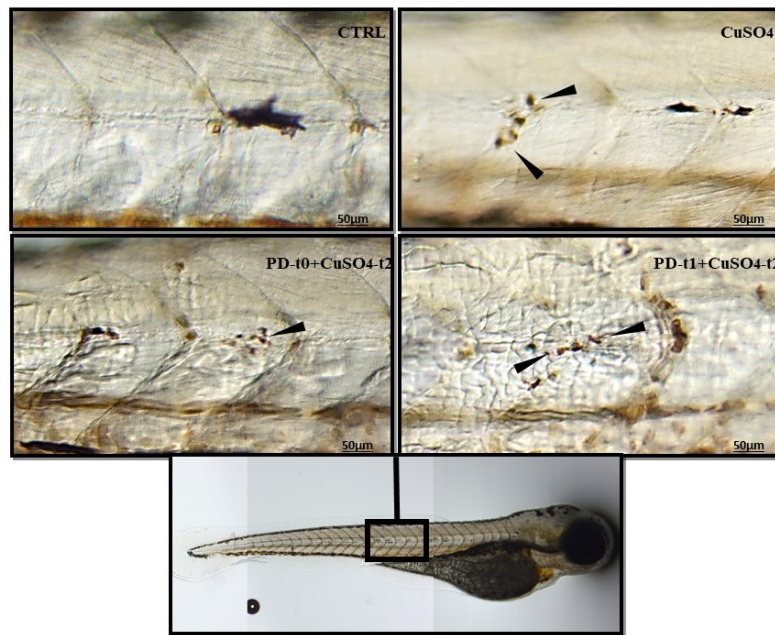


Fig.4.6.b The figure shows representative images of neutrophil migration in larvae lateral line. Photos represent the four experimental groups: control group larvae (CTRL), larvae treated only with copper sulfate (CuSO_4), larvae treated with polydatin for 3 hours before copper exposure (PD-t0 + CuSO_4 -t2) and larvae treated with polydatin for 1 hour before copper exposure (PD-t1+ CuSO_4 -t2). In the lower part of the panel, a larva in its entirety indicating the portion on which we have focused to capture the images of the lateral line. Neutrophils are indicated by black arrow. Scale 50 μm .

To optimize the pre exposure to polydatin, 2 times were used 1 hour and 3 hour. In control group there aren't neutrophils either in the heads (4.6.a) or in the lateral line (4.6.b). Larvae of the CuSO_4 group have a massive migration of neutrophils both in the head (4.6.a) and in the lateral line (4.6.b). Larvae of the

PD-t0+CuSO₄-t2 group exhibit lower neutrophil migration than the CuSO₄ group in the head (4.6.a) and in the lateral line (4.6.b). The larvae instead of the PD-t1+CuSO₄-t2 group exhibit lower neutrophil migration than CuSO₄ group but higher than the PD-t0+CuSO₄-t2 group in the head (4.6.a) and in lateral line (4.6.b).

For this reason, in our experiment for study immune response through neutrophil migration we sampled one hour later from the end of copper exposure and we decided to do a polydatin treatment for 3 hours before copper exposure. These two tests led to the decision of the timing of our experimental design (Fig. 3.1).

4.2.3 MPO TEST – CuSO₄ experiment

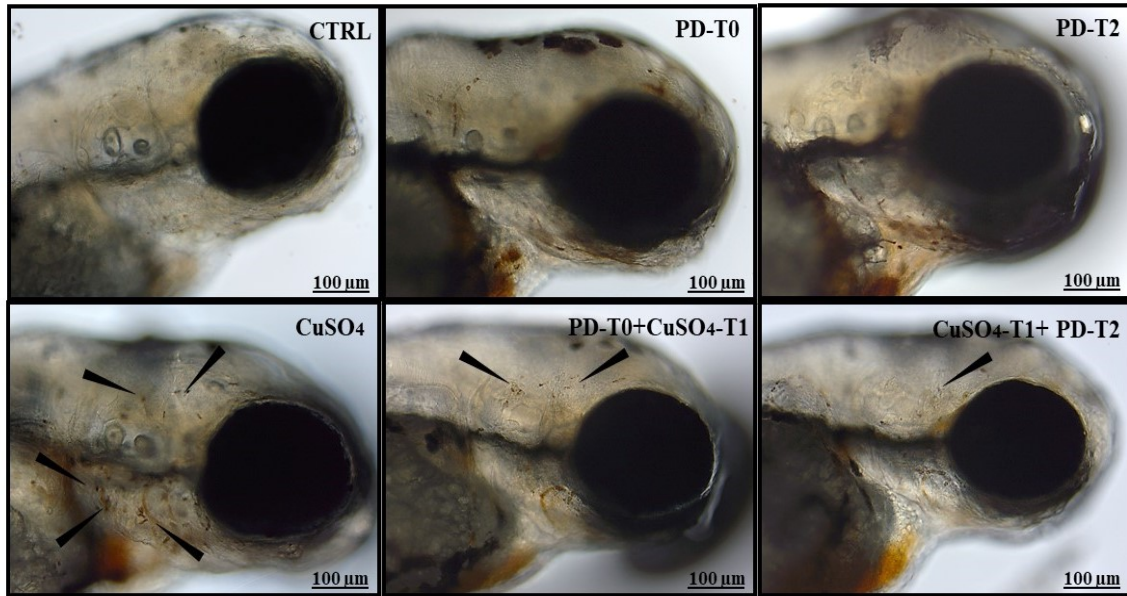


Fig. 4.7.a The figure shows representative images of neutrophil migration in the head of larvae sampled at T3. Photos represent the 6 experimental groups: control larvae (CTRL), larvae treated only with copper sulfate (CuSO₄), larvae treated with polydatin alone (PD-T0 and PD-T2), larvae treated with polydatin before copper exposure (PD+CuSO₄) and larvae treated with polydatin after copper exposure (CuSO₄+PD). Neutrophils are indicated with black arrows. Scale 100 μm.

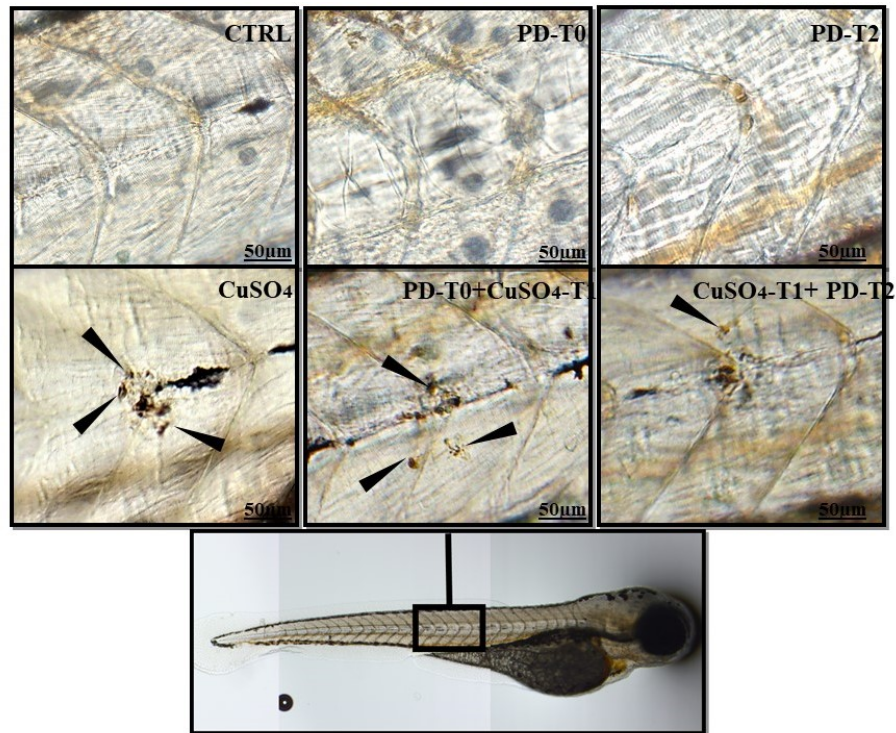


Fig.4.7.b The figure shows representative images of neutrophil migration in lateral line of larvae sampled at T3. Photos represent the 6 experimental groups: control larvae (CTRL), larvae treated only with copper sulfate (CuSO_4), larvae treated with polydatin alone (PD-T0 and PD-T2), larvae treated with polydatin before copper exposure (PD+ CuSO_4) and larvae treated with polydatin after copper exposure (CuSO_4 +PD). In the lower center there is a larva in its entirety which indicates the portion on which we have concentrated to capture the images of the lateral line. Neutrophils are indicated with black arrows. Scale 50 μm .

From Figures 4.7, panel a and b, it emerges that there is no migration of neutrophils in the head (4.7.a CTRL, PD-T0 and PD-T2) and in the lateral line

(4.7.b CTRL, PD-T0 and PD-T2) of the control group larvae as well as in larvae treated with polydatin alone. In larvae treated only with copper sulphate there is a massive presence of neutrophils both at the level of the head (4.7.a) and at the level of the lateral line (4.7.b). In larvae treated with polydatin for 3 hours before copper sulphate exposure, a lower neutrophil migration is noted both at the level of the head (4.7.a PD+CuSO₄) and at the level of the lateral line (4.7.b PD+CuSO₄). Larvae treated with polydatin for one hour after copper sulphate exposure show a migration less massive at the level of the head (4.7.a CuSO₄+PD) and at the level of the tail (4.7.b CuSO₄+PD) respect to CuSO₄ and PD+CuSO₄ groups.

4.2.4 MPO TEST- Cut tail experiment

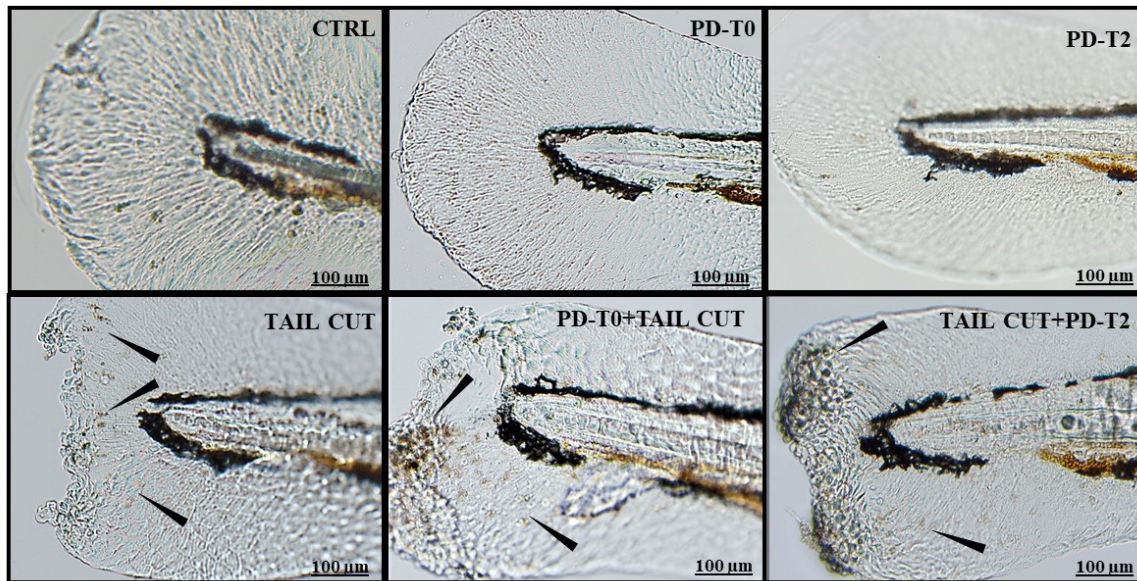


Fig.4.8 The figure shows representative images of neutrophil migration in caudal fin of larvae sampled at T3. Photos represent 6 experimental groups: control larvae (CTRL), larvae with cut of the caudal fin (TAIL CUT), larvae treated with polydatin alone (PD-T0 and PD-T2), larvae treated with polydatin before caudal fin cut (PD+TAIL CUT) and larvae treated with polydatin after caudal fin cut (TAIL CUT+PD). Neutrophils are indicated with black arrows. Scale 100 µm.

From figures 4.8 it emerges that there is no migration of neutrophils in the caudal fin in control group larvae and in larvae treated with polydatin alone. In larvae with caudal fin cut (4.8 TAIL CUT) there is a massive presence of neutrophils. In larvae treated with polydatin for 3 hours before caudal fin cut presents a massive neutrophil migration while larvae treated with polydatin for

one hour after caudal fin cut show a lower neutrophils migration respect to TAIL CUT and PD+TAIL CUT groups.

4.3 DASPEI STAINING

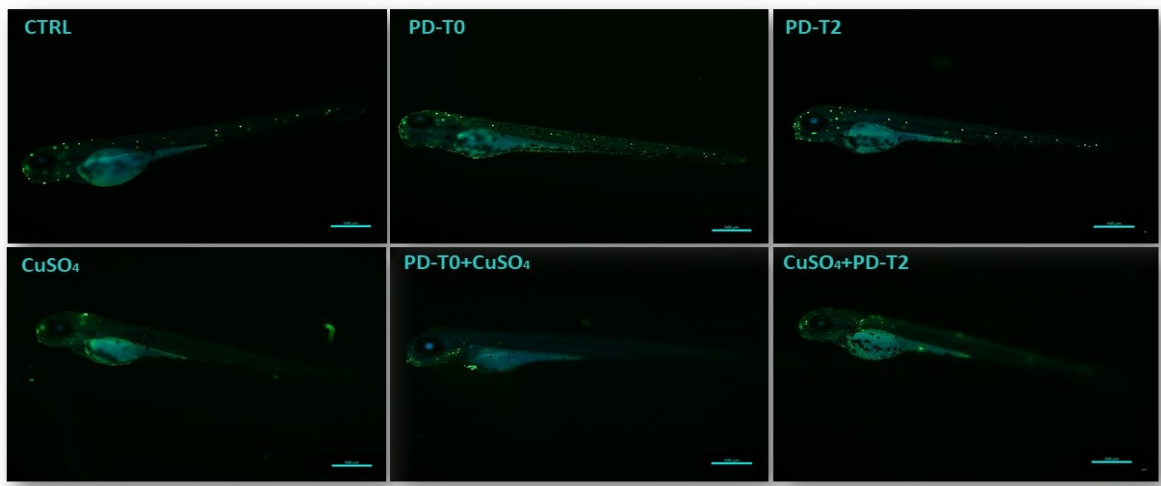


Fig.4.9 Picture shows lateral line neuromast (in fluorescence) in larvae sampled at time T3. The photos represent the 6 experimental groups: control larvae (CTRL), larvae treated only with copper sulfate (CuSO_4), larvae treated with polydatin alone (PD-T0 and PD-T2), larvae treated with polydatin before copper exposure (PD+ CuSO_4) and larvae treated with polydatin after copper exposure (CuSO_4 +PD). Scale 500 μm .

From Figures 4.9 the lateral line neuromast are present in the control group larvae and in larvae treated with polydatin alone. In all other experimental groups lateral line hair cells were destroyed.

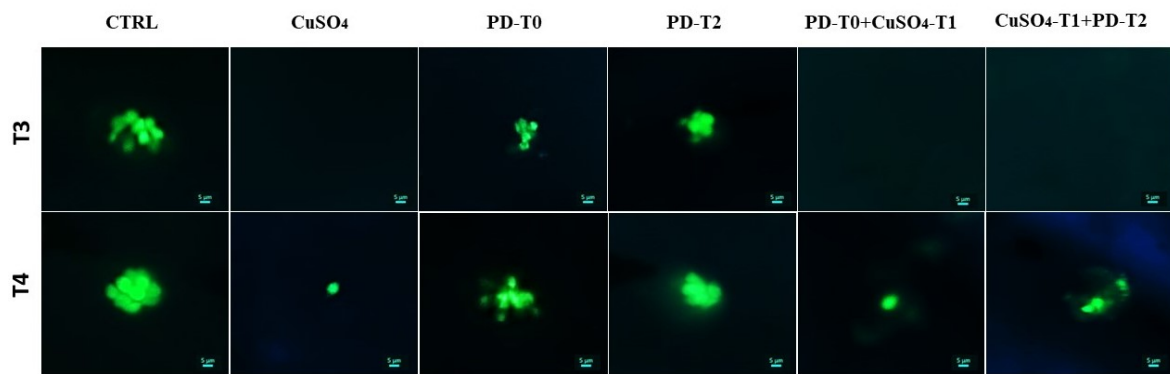


Fig.4.10 DASPEI staining high magnification of L1 neuromast (in fluorescence) in larvae sampled at time T3 (top line) and T4(lower line). Photos represent the 6 experimental groups from the left to the right: control larvae (CTRL), larvae treated with copper sulfate (CuSO_4), larvae treated with polydatin alone (PD-T0 and PD-T2), larvae treated with polydatin before copper exposure (PD+ CuSO_4) and larvae treated with polydatin after copper exposure (CuSO_4 +PD). Scale 5 μm .

Figure 4.10 shows that there are no relevant variations of L1 neuromast between T3 and T4 in CTRL, PD-T0 and PD-T2 groups larvae. The different staining between T3 and T4 of PD-T0 and PD-T2 groups is probably due to a different stage of hair cells maturation. In CuSO_4 , PD+ CuSO_4 and CuSO_4 +PD groups at T4 the neuromast first hair cells are noted to be regenerated.

4.4 Semiquantitative RT-PCR

4.4.1 Inflammation pathway

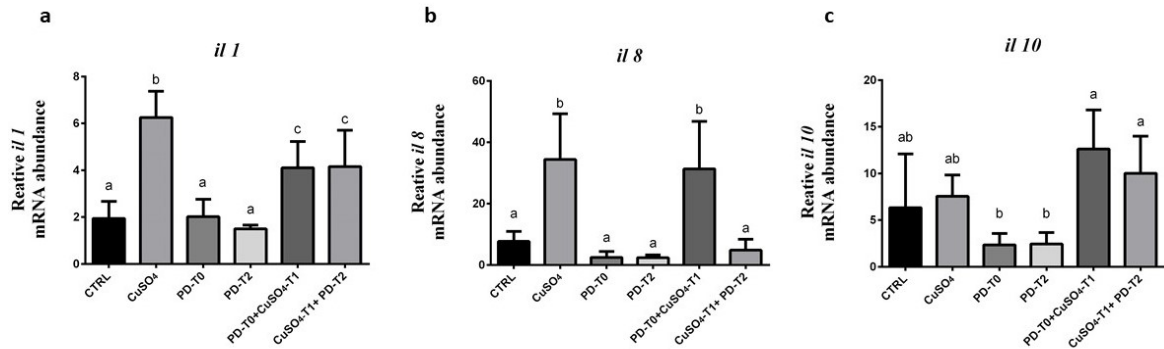


Fig.4.11 Relative mRNA abundance of *il1* (a), *il8* (b) and *il10* (c) in 6 experimental groups: control larvae (CTRL), larvae treated only with copper sulphate (CuSO₄), larvae treated with polydatin alone (PD-T0 and PD-T2), larvae treated with polydatin before copper exposure (PD+CuSO₄) and larvae treated with polydatin after copper exposure (CuSO₄+PD). Letters indicate significant differences (p < 0.05).

Figure 4.11, panel a, shows that the groups treated with copper sulphate (CuSO₄, PD+CuSO₄, CuSO₄+PD) show a significant increase in the expression of *il1* compared to the control, however the two experimental groups treated with polydatin before and after copper exposure present a 1/3 lower expression than the experimental group treated only with CuSO₄. The 2 groups treated only with PD the cytokine levels are similar to CTRL.

Figure 4.11, panel b, shows that gene expression of *il8* significantly increases only in the CuSO₄ and PD+CuSO₄ groups compared to all the other groups, but they show no differences between them. No other significant differences were detected among the other groups

Figure 4.11, panel c, shows that no differences are present between *il10* expression of CTRL, CuSO₄, PD-T0 and PD-T2 group. The only significant differences are between PD groups and groups treated with PD and CuSO₄, in this case, the PD groups show *interleukin10* expression of 2 times lower compared to groups treated with both substance, PD and CuSO₄. Polydatin treatments before and after copper exposure allow an increase in *il10* expression compared to CuSO₄ group. However, the increase is not significant and probably this is due to the high standard deviation values caused by biological variability.

4.4.2 Oxidative stress pathway

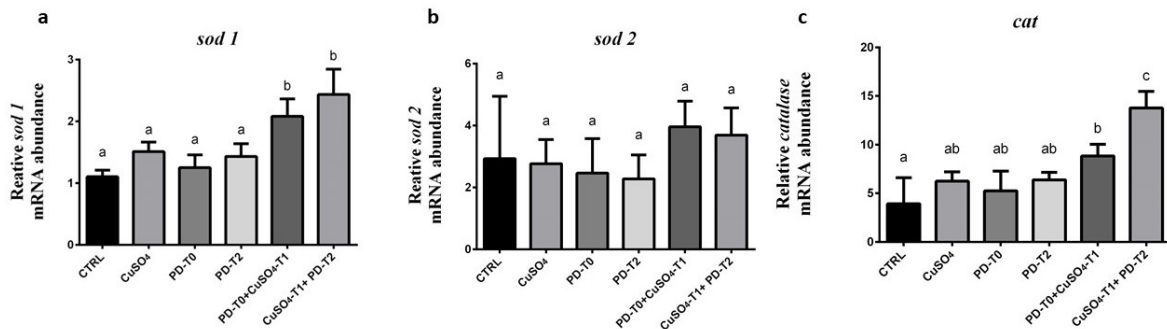


Fig.4.12 Relative mRNA abundance of *sod1* (a), *sod2* (b) and *cat* (c) in 6 experimental groups: control larvae (CTRL), larvae treated only with copper sulphate (CuSO₄), larvae treated with polydatin alone (PD-T0 and PD-T2), larvae treated with polydatin before copper exposure (PD+CuSO₄) and larvae treated with polydatin after copper exposure (CuSO₄+PD). Letters indicate significant differences (p < 0.05).

In Figure 4.12, panel a, the CTRL, CuSO₄, PD-T0 and PD-T2 groups do not show significant differences of *sod1* expression between them. Polydatin treatments before and after copper sulphate exposure increase about 2 times *sod1* expression levels compared to all other experimental groups. There are no significant differences between PD+CuSO₄ and CuSO₄+PD.

No significant differences are between the various experimental groups in term of *sod2* expression, although there is a trend that shows the high expression

levels of *sod2* in PD+CuSO₄ and CuSO₄+PD compared to the rest of the experimental groups (Fig.4.12, panel b).

As for *sod1* also for *cat* there aren't significant differences between the groups CTRL, CuSO₄, PD-T0 and PD-T2. Treatment with polydatin before copper exposure (PD+CuSO₄) has significantly higher *cat* expression levels than the control but not significantly different respect to CuSO₄, PD-T0 and PD-T2. In polydatin treatment after copper exposure (CuSO₄+PD), *cat* expression levels are significantly higher respect to CTRL (3 times higher) and about 50% higher than in all other groups (Fig.4.12, panel c).

4.4.3 Apoptosis and autophagy pathway

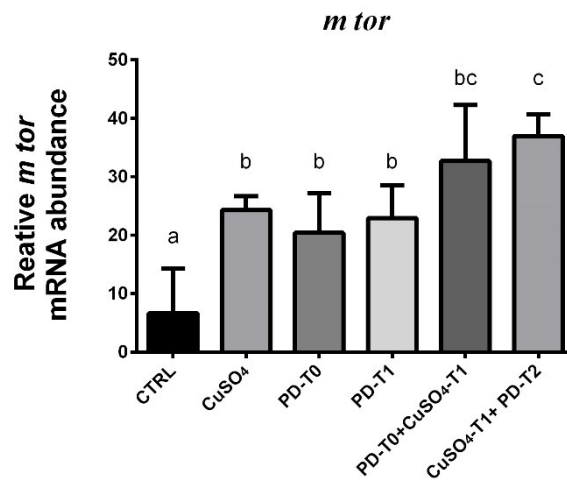


Fig.4.13 Relative mRNA abundance of *mtor* in 6 experimental groups: control larvae (CTRL), larvae treated only with copper sulphate (CuSO₄), larvae treated with polydatin alone (PD-T0 and PD-T2), larvae treated with polydatin before copper exposure (PD+CuSO₄) and larvae treated with polydatin after copper exposure (CuSO₄+PD). Letters indicate significant differences ($p < 0.05$).

In Figure 4.13 the treatment with copper sulphate evidence a significant increase (about two times) in the expression levels of *mtor* compared to the control group (CTRL). However, the expression levels of *mtor* in the groups treated with polydatin alone (PD-T0 and PD-T2) are significantly higher compared to the control but not significantly different with respect to treatment with CuSO₄. Treatment with polydatin before copper exposure has significantly 3 times higher levels of *mtor* expression than the control, however it is not

significantly different compared to the CuSO₄, PD-T0 and PD-T2 groups. In polydatin-treated group after copper exposure the expression levels of *mtor* are significantly about 3 times higher than in the CTRL, and about 50% higher than CuSO₄, PD-T0 and PD-T2 groups, but not significantly different from PD+CuSO₄.

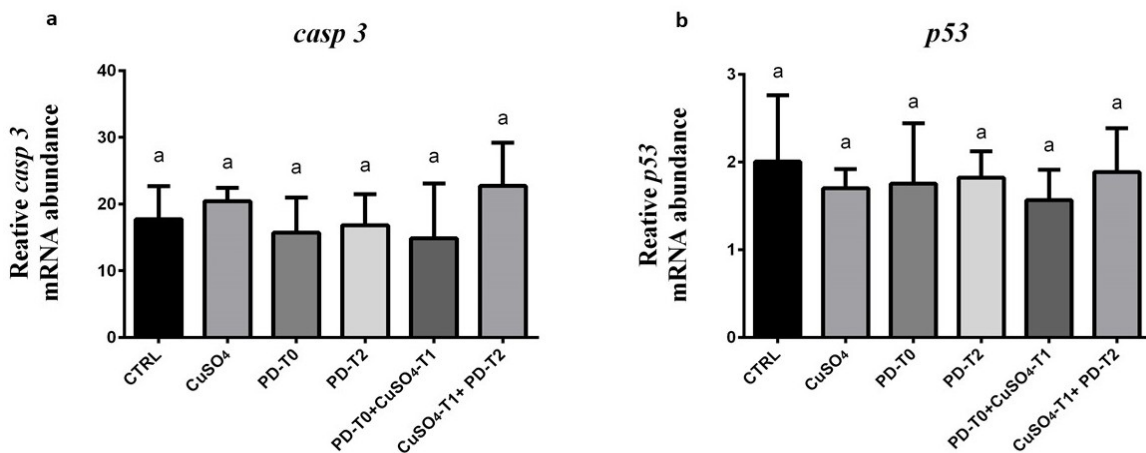


Fig.4.14 Relative mRNA abundance of *casp3* (a) and *p53* (b) in 6 experimental groups: control larvae (CTRL), larvae treated only with copper sulphate (CuSO₄), larvae treated with polydatin alone (PD-T0 and PD-T2), larvae treated with polydatin before copper exposure (PD+CuSO₄) and larvae treated with polydatin after copper exposure (CuSO₄+PD). Letters indicate significant differences ($p < 0.05$).

No differences in term of *casp3* and *p53* expression between the various experimental groups in both figures (4.13, panel a and b).

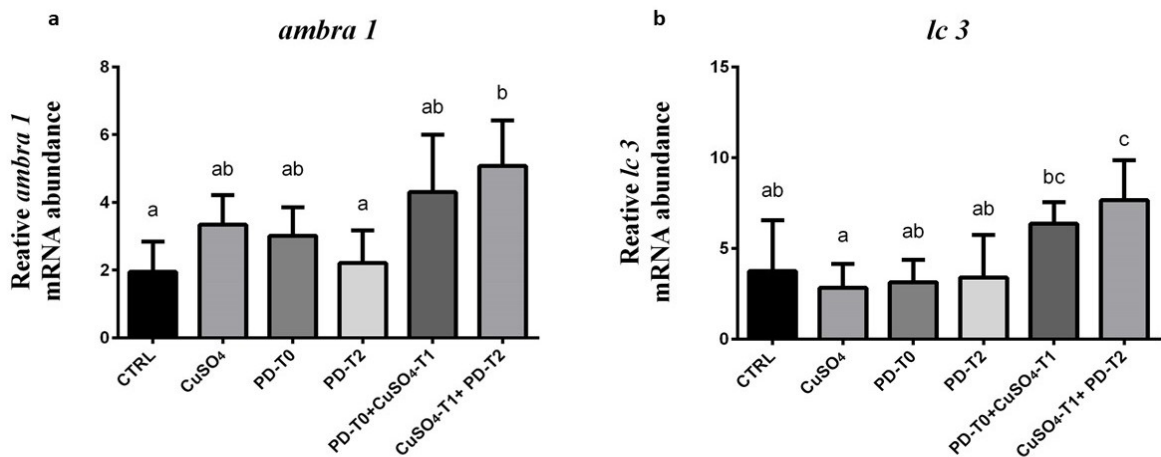


Fig.4.15 Relative mRNA abundance of *ambra1* (a) and *lc3* (b) in 6 experimental groups: control larvae (CTRL), larvae treated only with copper sulphate (CuSO₄), larvae treated with polydatin alone (PD-T0 and PD-T2), larvae treated with polydatin before copper exposure (PD+CuSO₄) and larvae treated with polydatin after copper exposure (CuSO₄+PD). Letters indicate significant differences (p < 0.05).

Likewise to *sod1*, *sod2* and *cat* no significant differences in the expression levels of *ambra1* and *lc3* between the CTRL, CuSO₄, PD-T0 and PD-T2 groups were detected (Figure 4.15). Although there are not always significant differences, the increase of expression in the treated experimental groups seems to be confirmed also for *ambra1* and *lc3* in treatment with PD before and after copper exposure.

Among the groups treated with polydatin before and after copper exposure there are no significant differences in term of expression of *ambra1*, at the same

time the CuSO₄+PD group is significantly higher (about 3 times higher) than the control (Figure 4.15, panel a).

The increase in *lc3* expression of the CuSO₄+PD group respect to the control is smaller than in *ambra1*, but it remains significant (Figure 4.15, panel b).

4.4.4 Neuromast regeneration pathway

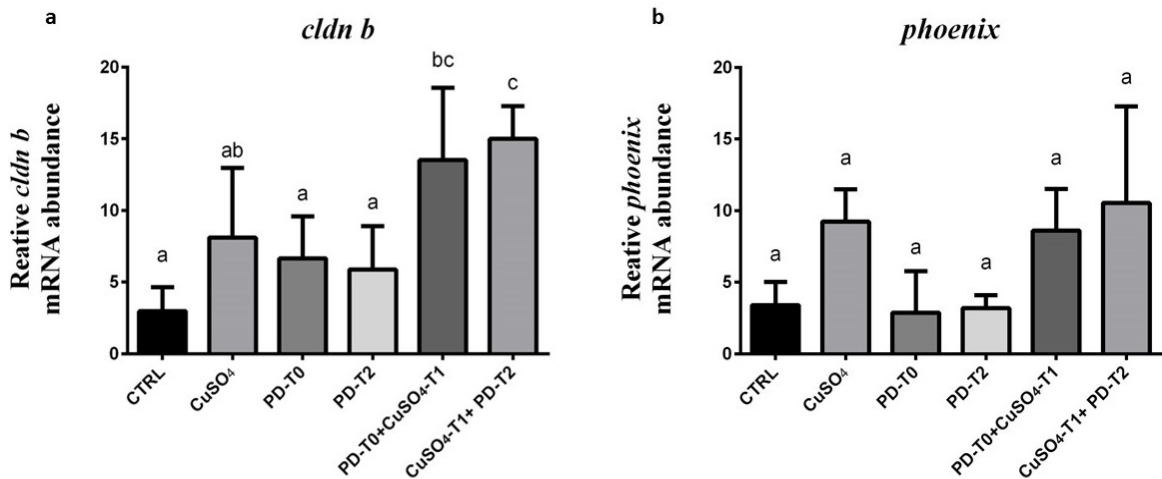


Fig.4.16 Relative mRNA abundance of *cldn b* (a) and *phoenix* (b) in 6 experimental groups: control larvae (CTRL), larvae treated only with copper sulphate (CuSO₄), larvae treated with polydatin alone (PD-T0 and PD-T2), larvae treated with polydatin before copper exposure (PD+CuSO₄) and larvae treated with polydatin after copper exposure (CuSO₄+PD). Letters indicate significant differences ($p < 0.05$).

Figure 4.16, panel a, shows that there are no significant differences in the CTRL, CuSO₄, PD-T0 and PD-T2 groups. The expression levels of the

PD+CuSO₄ group are significantly higher (about 3 times) compared to the CTRL, PD-T0 and PD-T2 groups, but they are not significantly different compared to the CuSO₄ group even if the trend seems higher. The expression levels of *cldn b* in the CuSO₄+PD group are significantly higher (3 times) than in all other groups.

Figure 4.16, panel b, shows the expression levels of *phoenix*. From the image we can see that there are no significant differences between the various experimental groups, although from the trend of expression levels we can see that the levels of the CuSO₄, PD+CuSO₄ and CuSO₄+PD groups are higher than the CTRL, PD-T0 and PD-T2 groups.

4.4.5 Proliferation pathway

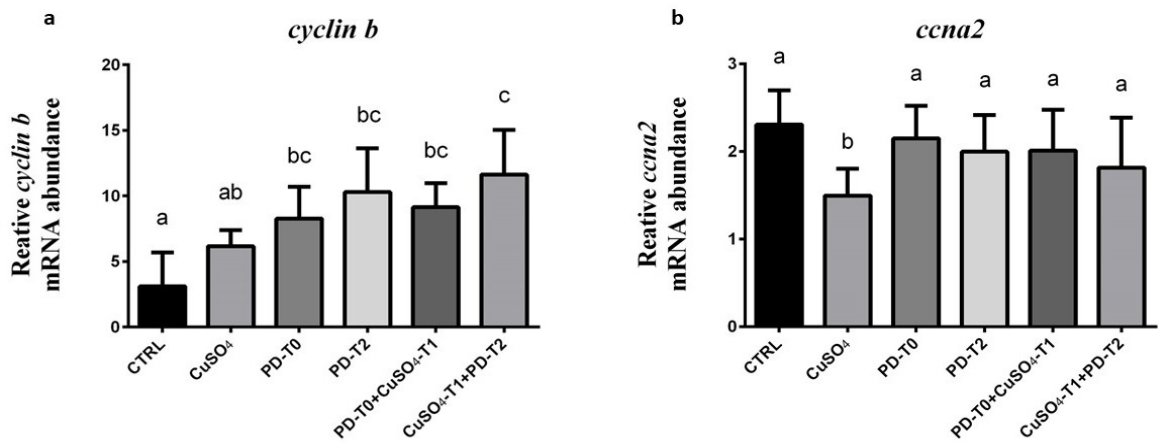


Fig.4.17 Relative mRNA abundance of *cyclin b* (a) and *ccna2* (b) in 6 experimental groups: control larvae (CTRL), larvae treated only with copper sulphate (CuSO₄), larvae treated with polydatin alone (PD-T0 and PD-T2), larvae treated with polydatin before copper exposure (PD+CuSO₄) and larvae treated with polydatin after copper exposure (CuSO₄+PD). Different letters indicate significant differences (p < 0.05).

Related to *cyclin b* expression there are no significant differences between the group CuSO₄ and CTRL even if CuSO₄ shows a slightly higher trend. The PD-T0, PD-T2 and PD+CuSO₄ groups are significantly higher than the control but not compared to CuSO₄. Only CuSO₄+PD group is significantly higher (about 3 times) than the CTRL and CuSO₄ (Fig.4.17, panel a).

Only CuSO₄ groups show a variation in *ccna2* expression that is significantly lower than the rest of the experimental groups (Fig. 4.17 panel b).

5. DISCUSSION

This study allowed us to evaluate the efficacy of polydatin administered in a preventive or curative manner in conditions of chemical damage, due to CuSO₄ exposure, or mechanical damage, due to caudal fin cut. This study was conducted in zebrafish, due to its innumerable characteristics that make it an excellent experimental model (Khan and Alhewairini, 2018) for the study of substances such as polydatin which in recent years has captured a great scientific interest in biomedical research.

Polydatin anti-inflammatory effects

Through the myeloperoxidase test, a relatively simple and fast technique, it was possible to verify polydatin effect on the zebrafish immune system. Results (Figures 4.7.a and 4.7.b) showed that polydatin treatments is associated to lower neutrophil migration in larvae of PD+CuSO₄ and CuSO₄+PD groups compared to larvae treated with copper sulphate alone. Therefore, these results indicated that polydatin treatments allows a greater defense against oxidative stress induced by copper sulphate, with consequent lower activation of the inflammatory response. Furthermore, the test also showed that neutrophils migration in larvae treated with polydatin for 1h after copper sulphate exposure is lower than in larvae treated with polydatin for 3h before copper exposure

indicating that the antioxidant effects of polydatin is strong if administered after the stressor. Results of *il8* gene expression, a gene involved in neutrophils chemotaxis (Xu Z et al, 2019), supported this hypothesis, in fact, from the results obtained by the RT-PCR (Fig. 4.11, panel b) it is evident as the treatment with polydatin for 1 hour after copper exposure significantly lowered *il8* expression levels compared to both the group of larvae treated with copper sulphate alone and larvae treated with polydatin for 3 h before copper exposure. Other signals involved in immune responses such as, *il1* and *il10* were studied to evaluate anti-inflammatory activity of polydatin. The *il1*, expressed through NF-kB activation by the cells following ROS accumulation induced by oxidative damage, (Liu et al., 2017), presents a similar trend of *il8* expression (Fig.4.11, panel b), even if in this case both polydatin treatments before and after copper exposure significantly lowered *il1* levels compared to CuSO₄ group evidencing no differences when polydatin was used as preventive or as curative treatment. On the other hand, in the PD+CuSO₄ and CuSO₄+PD groups, polydatin increased *il10* expression, a gene with anti-inflammatory activity that modulates proinflammatory cytokines expression to defense the cells from immune system hyperactivation. These different trends were due to the different action carried out by the different cytokines (Boraschi and Tagliavue, 1996; Hammond et al., 1995; Mosser 2008), in fact, polydatin

treatments allowed a lower activation of the immune system by modulating the expression of the pro-inflammatory cytokines *il1* and *il8*, and *il10*.

The polydatin is effective also in case of mechanical stress, in fact, we performed a myeloperoxidase test in larvae in which the inflammation had been induced by the caudal fin cut (section 3.2). Similarly, these results (Fig.4.8) confirmed that polydatin treatments before and after caudal fin cut allow a lower migration of neutrophils compared to the group of larvae in which the caudal fin was cut and not subjected to any type of treatment. We can therefore hypothesize that the polydatin had anti-inflammatory properties both if administered before the induction of inflammation as well as if administered after the stress. However, the administration of polydatin after the induction of inflammation, even if for a shorter time, seems to have a greater effect, lowering the expression levels of *il8* and consequently reducing the migration of neutrophils in the site of damage evidencing a clear anti-inflammatory action.

Polydatin anti-oxidant effects

Response to oxidative stress was evaluated by studying the expression of the *sod1*, *sod2* and *cat*. ROS accumulation inside the cell leads to the activation of NF-kB which allows the transcription of *sod* and *cat* (section 1.3.1), genes codifying for enzymes involved in the response to oxidative stress inside the

cell (Ighodaro and Akinloye, 2018; Chelikani et al., 2004). From results obtained by RT-PCR (4.12) we found that the polydatin treatments before and after copper exposure allowed a significant increase in the expression levels of *sod1* and *cat* compared to the rest of the experimental groups including the CuSO₄ group. These results indicated that polydatin allowed greater transcription of genes with antioxidant activity to better counteract the damage induced by ROS excess. The *sod1* and *cat* expression levels were higher in polydatin treatments after copper exposure, again indicating that the polydatin administered after induction of oxidative stress allowed a greater response. The *sod2* shows a similar trend of *sod1* and *cat* although the expression levels of *sod2* in polydatin treated before and after copper exposure were not significant among the groups. This difference in expression can be due to the different localization of *sod* in cellular compartments, in fact, it is known that *sod1* is found in the cytosol, while *sod2* in the mitochondria (Fridovich, 1995). A different stimulation of this gene by CuSO₄ may suggest that toxic effects of copper are more explicit in cytosol than in mitochondria.

Polydatin effects in apoptosis and autophagy processes

ROS excess can lead the cell to react through apoptotic or autophagic processes depending on the concentration of ROS generated (Gibson, 2013). To understand whether apoptotic or autophagic processes were induced in our

experiment, we first studied *mtor* gene expression (Fig.4.13), usually involved in the regulation of the two processes, and subsequently we compared its expression with *p53* and *casp3* genes expression levels, involved in the apoptotic process (McIlwain et al., 2013; Finlay et al., 1989), and *ambra1* and *lc3* genes expression levels, involved in autophagic process (Fimia et al., 2013; Klionsky et al., 2016; Nguyen et al., 2016).

While *mtor* expression increased significantly in all treated groups compared to the control and its concentration is highest in groups treated with both PD and CuSO₄ (Fig.4.13), *p53* and *casp3* expressions did not show significant differences among the groups (Fig.4.14). On the other hand, expression levels of *ambra1* and *lc3*, showed the same trend of *mtor*, so expression levels significantly increase in polydatin treatments before and after copper exposure. Generally, high expression of *mtor* blocks the autophagic processes (Rabanal-Ruiz et al., 2017) and so we expected to see changes only in the genes involved in apoptotic processes, therefore, the increase of genes related to autophagy may be due to autophagy pathway independent to *mtor* signals. These results indicate that polydatin treatments before and after stress induction allow better cell recovery through autophagic processes compared to copper sulphate treatments.

Polydatin effects in cell growth and proliferation process

mtor may also be involved in cell cell growth and proliferation processes (Kraft, 2016) so that the expression of genes, as *cyclin b* and *ccna2* were analyzed to better understand the expression pattern of *mtor*. The trend of expression of *cyclin b* (Fig.4.17) was similar to *mtor* expression and the main significant changes of expression, compared to the control group, occurred in the groups treated with PD before and after copper exposure; so, we hypothesize that the increase of *mtor* is implicated in proliferative processes and not in apoptotic processes. Proliferative processes can therefore be induced either by exposure to copper or by exposure to polydatin, increasing even more cell division when both treatments were performed. Differently from *cyclin b*, *ccna2* expression did not present significant differences except in treatments with copper sulphate which was significantly lower than the rest of experimental groups (Fig.4.17, panel b). Indeed, levels of *cyclin b* were expressed during cell cycle mitosis, while the levels of *ccna* reached the apex in the G2 phase of cell cycle.

Polydatin effects in hair cells regeneration

Through a qualitative analysis based on the DASPEI staining, shown in Figure 4.9, we observed that exposure to copper induced the destruction of all lateral line hair cell neuromasts. Treatment with polydatin before exposure to copper

did not prevented necrosis of lateral line hair cells. However, analysis to evaluate the regeneration of L1 hair cell neuromast after 24 hours carried out with DASPEI staining showed an improved regenerative process in larvae treated with polydatin after copper exposure (Fig.4.10). In addition to DASPEI staining, we studied the regenerative processes by the *cldnb* and *phoenix* genes expression both expressed in neuromast supporting cells and involved in regeneration processes (Behra et al., 2009; Sonnack et al., 2018). The expression of these genes was increased in polydatin treatments before and after copper exposure compared to other groups. These results make us hypothesize that polydatin could accelerate the regenerative processes of lateral line cells.

Polydatin effects on zebrafish development

From the morphological analyzes reported in paragraph 4.1 we found that the larvae exposed to copper sulphate showed a developmental delay, in particular, larvae presented an incorrect swim bladder insufflation, deformity and lower growth. Results showed that polydatin treatments before and after copper exposure allow a recovery of developmental and growth process. In fact, larvae treated with polydatin before and after copper exposure showed a correct insufflation of swim bladder in the 31% and 57% respectively (Fig.4.3). Copper exposure induces dorsal curvatures in 78% of zebrafish larvae, but, polydatin

treatment before and after copper exposure reduced the percentage of scoliosis at 43% and 30% respectively (Fig.4.4). Furthermore, polydatin treatments allowed a recovery of growth (Fig.4.2, panel c) providing clear evidences on the positive effects of polydatin in the developmental process preventing deformities induced by chemical stress.

6. CONCLUSIONS AND FUTURE PERSPECTIVES

This study clearly showed how polydatin helps the cell to compensate for damage caused by oxidative stress by modulating cellular inflammation, antioxidant and autophagic response. In particular, it would seem that a curative administration of polydatin produces better effects compared to a preventive administration. We also found that polydatin allows greater cell proliferation and improve regenerative processes of the hair cells of the lateral line after being damaged by CuSO_4 . Results obtained provided numerous answers on the mechanism of action of polydatin, but at the same time many other questions remained open. In the future we will try to understand if the proliferative activity induced by polydatin is linked to the growth of the larva by studying for example the expression levels of GH and other signals of the growth pathway. Other analyzes will aim to understand how polydatin can improve the regeneration of neuromast hair cells and whether its proliferative activity can also be involved in these regenerative processes by localizing the expression of genes involved in neuromast proliferation process.

BIBLIOGRAPHY

Balasubramanian, Shankar, and Stephen Neidle. "G-quadruplex nucleic acids as therapeutic targets." *Current opinion in chemical biology* 13.3 (2009): 345-353.

Ban, Suk-Ho, et al. "Effects of a bio-assay guided fraction from *Polygonum cuspidatum* root on the viability, acid production and glucosyltransferase of mutans streptococci." *Fitoterapia* 81.1 (2010): 30-34.

Behra, Martine, et al. "Phoenix is required for mechanosensory hair cell regeneration in the zebrafish lateral line." *PLoS genetics* 5.4 (2009): e1000455.

Bergmann, Andreas, and Hermann Steller. "Apoptosis, stem cells, and tissue regeneration." *Sci. Signal.* 3.145 (2010): re8-re8.

Bonucci, Massimo, et al. "Integrated cancer treatment in the course of metastatic pancreatic cancer: complete resolution in 2 cases." *Integrative cancer therapies* 17.3 (2018): 994-999.

Boraschi, Diana, and Aldo Tagliabue. "The interleukin-1 receptor family." *Vitamins & Hormones* 74 (2006): 229-254.

Campo, Pierre, Thais C. Morata, and OiSaeng Hong. "Chemical exposure and hearing loss." *Disease-a-month: DM* 59.4 (2013): 119.

Chelikani, Prashen, Ignacio Fita, and Peter C. Loewen. "Diversity of structures and properties among catalases." *Cellular and Molecular Life Sciences CMLS* 61.2 (2004): 192-208.

Chen, Yupin, et al. "Anti-oxidant polydatin (piceid) protects against substantia nigral motor degeneration in multiple rodent models of Parkinson's disease." *Molecular neurodegeneration* 10.1 (2015): 4.

Chitnis, Ajay B., Damian Dalle Nogare, and Miho Matsuda. "Building the posterior lateral line system in zebrafish." *Developmental neurobiology* 72.3 (2012): 234-255

Crosby, Meredith E. "Cell cycle: principles of control." *The Yale Journal of Biology and Medicine* 80.3 (2007): 141.

- d'Alençon, Claudia A., et al. "A high-throughput chemically induced inflammation assay in zebrafish." *BMC biology* 8.1 (2010): 151.
- d'Amelio, Marcello, et al. "Caspase-3 triggers early synaptic dysfunction in a mouse model of Alzheimer's disease." *Nature neuroscience* 14.1 (2011): 69.
- Darrow, Kiersten O., and William A. Harris. "Characterization and development of courtship in zebrafish, *Danio rerio*." *Zebrafish* 1.1 (2004): 40-45.
- Denton, Donna, and Sharad Kumar. "Autophagy-dependent cell death." *Cell Death & Differentiation* (2018): 1.
- Du, Qiao-Hui, Cheng Peng, and Hong Zhang. "Polydatin: a review of pharmacology and pharmacokinetics." *Pharmaceutical biology* 51.11 (2013): 1347-1354.
- Engeszer, Raymond E., et al. "Timing and plasticity of shoaling behaviour in the zebrafish, *Danio rerio*." *Animal behaviour* 74.5 (2007): 1269-1275.
- Fabris, Sabrina, et al. "Antioxidant properties of resveratrol and piceid on lipid peroxidation in micelles and monolamellar liposomes." *Biophysical chemistry* 135.1-3 (2008): 76-83.
- Ferri, Karine F., and Guido Kroemer. "Organelle-specific initiation of cell death pathways." *Nature cell biology* 3.11 (2001): E255.
- Fimia, G. M., et al. "Ambra1 at the crossroad between autophagy and cell death." *Oncogene* 32.28 (2013): 3311.
- Finlay, Cathy A., Philip W. Hinds, and Arnold J. Levine. "The p53 proto-oncogene can act as a suppressor of transformation." *Cell* 57.7 (1989): 1083-1093.
- Fischer, Roman, and Olaf Maier. "Interrelation of oxidative stress and inflammation in neurodegenerative disease: role of TNF." *Oxidative medicine and cellular longevity* 2015 (2015).
- Fraher, Daniel, et al. "Zebrafish embryonic lipidomic analysis reveals that the yolk cell is metabolically active in processing lipid." *Cell reports* 14.6 (2016): 1317-1329.
- Fridovich, Irwin. "Superoxide radical and superoxide dismutases." *Annual review of biochemistry* 64.1 (1995): 97-112.

- Gaetke, Lisa M., Hannah S. Chow-Johnson, and Ching K. Chow. "Copper: toxicological relevance and mechanisms." *Archives of toxicology* 88.11 (2014): 1929-1938.
- Gemberling, Matthew, et al. "The zebrafish as a model for complex tissue regeneration." *Trends in Genetics* 29.11 (2013): 611-620.
- Ghysen, Alain, and Christine Dambly-Chaudiere. "Development of the zebrafish lateral line." *Current opinion in neurobiology* 14.1 (2004): 67-73.
- Gibson, Spencer B. "Investigating the role of reactive oxygen species in regulating autophagy." *Methods in enzymology*. Vol. 528. Academic Press, 2013. 217-235.
- Gompel, Nicolas, et al. "Pattern formation in the lateral line of zebrafish." *Mechanisms of development* 105.1-2 (2001): 69-77.
- González-Polo, Rosa-Ana, et al. "The apoptosis/autophagy paradox: autophagic vacuolization before apoptotic death." *Journal of cell science* 118.14 (2005): 3091-3102.
- Goolish, E. M., Okutake, K., & Lesure, S. (1999). Growth and survivorship of larval zebrafish *Danio rerio* on processed diets. *North American Journal of Aquaculture*, 61(3), 189-198.
- Green, Douglas R., and Fabien Llambi. "Cell death signaling." *Cold Spring Harbor perspectives in biology* 7.12 (2015): a006080.
- Haehnel, Melanie, Masashige Taguchi, and James C. Liao. "Heterogeneity and dynamics of lateral line afferent innervation during development in zebrafish (*Danio rerio*)." *Journal of Comparative Neurology* 520.7 (2012): 1376-1386.
- Halliwell, Barry. "Free radicals and antioxidants—quo vadis?." *Trends in pharmacological sciences* 32.3 (2011): 125-130.
- Hammond, M. E., et al. "IL-8 induces neutrophil chemotaxis predominantly via type I IL-8 receptors." *The Journal of Immunology* 155.3 (1995): 1428-1433.
- Hay, Nissim, and Nahum Sonenberg. "Upstream and downstream of mTOR." *Genes & development* 18.16 (2004): 1926-1945.
- Harris, Julie A., et al. "Neomycin-induced hair cell death and rapid regeneration in the lateral line of zebrafish (*Danio rerio*)." *Journal of the Association for Research in Otolaryngology* 4.2 (2003): 219-234.

He, Y. D., et al. "Polydatin suppresses ultraviolet B-induced cyclooxygenase-2 expression in vitro and in vivo via reduced production of reactive oxygen species." *British Journal of Dermatology* 167.4 (2012): 941.

Henry, Caroline, et al. "Cellular uptake and efflux of trans-piceid and its aglycone trans-resveratrol on the apical membrane of human intestinal Caco-2 cells." *Journal of agricultural and food chemistry* 53.3 (2005): 798-803.

Henry-Vitrac, Caroline, et al. "Transport, deglycosylation, and metabolism of trans-piceid by small intestinal epithelial cells." *European journal of nutrition* 45.7 (2006): 376-382.

Herbomel, Philippe, Bernard Thisse, and Christine Thisse. "Ontogeny and behaviour of early macrophages in the zebrafish embryo." *Development* 126.17 (1999): 3735-3745.

Herbomel, Philippe, Bernard Thisse, and Christine Thisse. "Zebrafish early macrophages colonize cephalic mesenchyme and developing brain, retina, and epidermis through a M-CSF receptor-dependent invasive process." *Developmental biology* 238.2 (2001): 274-288.

Hernández, Pedro P., et al. "Regeneration in zebrafish lateral line neuromasts: Expression of the neural progenitor cell marker *sox2* and proliferation-dependent and-independent mechanisms of hair cell renewal." *Developmental neurobiology* 67.5 (2007): 637-654.

Hernández, Pedro P., and Miguel L. Allende. "Zebrafish (*Danio rerio*) as a model for studying the genetic basis of copper toxicity, deficiency, and metabolism." *The American journal of clinical nutrition* 88.3 (2008): 835S-839S.

Hernandez, Pedro P., et al. "Sublethal concentrations of waterborne copper induce cellular stress and cell death in zebrafish embryos and larvae." *Biological research* 44.1 (2011): 7-15.

Hordyjewska, Anna, Łukasz Popiołek, and Joanna Kocot. "The many "faces" of copper in medicine and treatment." *Biometals* 27.4 (2014): 611-621.

Huang, Zhao-Sheng, et al. "Protective effects of polydatin against CCl₄-induced injury to primarily cultured rat hepatocytes." *World journal of gastroenterology* 5.1 (1999): 41.

Ighodaro, O. M., and O. A. Akinloye. "First line defence antioxidants-superoxide dismutase (SOD), catalase (CAT) and glutathione peroxidase

(GPX): Their fundamental role in the entire antioxidant defence grid." *Alexandria Journal of Medicine* 54.4 (2018): 287-293.

Jaiser, Stephan R., and Gavin P. Winston. "Copper deficiency myelopathy." *Journal of neurology* 257.6 (2010): 869-881.

Ji, Hui, et al. "Polydatin modulates inflammation by decreasing NF- κ B activation and oxidative stress by increasing Gli1, Ptch1, SOD1 expression and ameliorates blood–brain barrier permeability for its neuroprotective effect in pMCAO rat brain." *Brain research bulletin* 87.1 (2012): 50-59.

Kerr, John FR, Andrew H. Wyllie, and Alastair R. Currie. "Apoptosis: a basic biological phenomenon with wideranging implications in tissue kinetics." *British journal of cancer* 26.4 (1972): 239.

Khan, Farmanur Rahman, and Saleh Alhewairini. "Zebrafish (*Danio rerio*) as a Model Organism." *Current Trends in Cancer Management*. IntechOpen, 2018.

Kim, Do-Hyung, et al. "mTOR interacts with raptor to form a nutrient-sensitive complex that signals to the cell growth machinery." *Cell* 110.2 (2002): 163-175.

Kim, Do-Hyung, et al. "Removal mechanisms of copper using steel-making slag: adsorption and precipitation." *Desalination* 223.1-3 (2008): 283-289.

Kimmel, Charles B., et al. "Stages of embryonic development of the zebrafish." *Developmental dynamics* 203.3 (1995): 253-310.

Klionsky, Daniel J., et al. "Guidelines for the use and interpretation of assays for monitoring autophagy." *Autophagy* 12.1 (2016): 1-222.

Kono, Hajime, and Kenneth L. Rock. "How dying cells alert the immune system to danger." *Nature Reviews Immunology* 8.4 (2008): 279.

Kumar, Neeraj, et al. "Copper deficiency myelopathy." *Archives of neurology* 61.5 (2004): 762-766.

Laale, Hans W. "The biology and use of zebrafish, *Brachydanio rerio* in fisheries research. A literature review." *Journal of Fish Biology* 10.2 (1977): 121-173.

La Fontaine, Sharon, M. Leigh Ackland, and Julian FB Mercer. "Mammalian copper-transporting P-type ATPases, ATP7A and ATP7B: emerging roles." *The international journal of biochemistry & cell biology* 42.2 (2010): 206-209.

Lai, Yuling, et al. "Polydatin alleviated alcoholic liver injury in zebrafish larvae through ameliorating lipid metabolism and oxidative stress." *Journal of pharmacological sciences* 138.1 (2018): 46-53.

Lawrence, Christian. "The husbandry of zebrafish (*Danio rerio*): a review." *Aquaculture* 269.1-4 (2007): 1-20.

Ledent, Bénédicte. *Caryl Phillips*. Manchester University Press, 2002.

Leite, Carlos Eduardo, et al. "Involvement of purinergic system in inflammation and toxicity induced by copper in zebrafish larvae." *Toxicology and applied pharmacology* 272.3 (2013): 681-689.

Li, Huihui, and Gu Yuan. "Electrospray ionization mass spectrometry probing of formation and recognition of the G-quadruplex in the proximal promoter of the human vascular endothelial growth factor gene." *Rapid Communications in Mass Spectrometry* 24.14 (2010): 2030-2034.

Li, Li, et al. "Live imaging reveals differing roles of macrophages and neutrophils during zebrafish tail fin regeneration." *Journal of Biological Chemistry* 287.30 (2012): 25353-25360.

Li, Run-Ping, et al. "Polydatin protects learning and memory impairments in a rat model of vascular dementia." *Phytomedicine* 19.8-9 (2012): 677-681.

Lieschke, Graham J., and Peter D. Currie. "Animal models of human disease: zebrafish swim into view." *Nature Reviews Genetics* 8.5 (2007): 353.

Liew, Woei Chang, and László Orbán. "Zebrafish sex: a complicated affair." *Briefings in functional genomics* 13.2 (2013): 172-187.

Lin, Lin, and Eric H. Baehrecke. "Autophagy, cell death, and cancer." *Molecular & cellular oncology* 2.3 (2015): e985913.

Lingappan, Krithika. "NF- κ B in oxidative stress." *Current opinion in toxicology* 7 (2018): 81-86.

Liu, Huanhai, et al. "Reactive oxygen species-mediated endoplasmic reticulum stress and mitochondrial dysfunction contribute to polydatin-induced apoptosis in human nasopharyngeal carcinoma CNE cells." *Journal of cellular biochemistry* 112.12 (2011): 3695-3703.

Liu, Ting, et al. "NF- κ B signaling in inflammation." *Signal transduction and targeted therapy* 2 (2017): 17023.

Lopez-Novoa, Jose M., et al. "New insights into the mechanism of aminoglycoside nephrotoxicity: an integrative point of view." *Kidney international* 79.1 (2011): 33-45.

López-Schier, Hernán, and A. J. Hudspeth. "A two-step mechanism underlies the planar polarization of regenerating sensory hair cells." *Proceedings of the National Academy of Sciences* 103.49 (2006): 18615-18620.

Ma, Eva Y., Edwin W. Rubel, and David W. Raible. "Notch signaling regulates the extent of hair cell regeneration in the zebrafish lateral line." *Journal of Neuroscience* 28.9 (2008): 2261-2273.

Mackenzie, Scott M., and David W. Raible. "Proliferative regeneration of zebrafish lateral line hair cells after different ototoxic insults." *PloS one* 7.10 (2012): e47257.

Maiuri, M. Chiara, et al. "Self-eating and self-killing: crosstalk between autophagy and apoptosis." *Nature reviews Molecular cell biology* 8.9 (2007): 741.

Malavolta, Marco, et al. "Serum copper to zinc ratio: Relationship with aging and health status." *Mechanisms of ageing and development* 151 (2015): 93-100.

Mariotti, Massimo, Marta Carnovali, and Giuseppe Banfi. "Danio rerio: the Janus of the bone from embryo to scale." *Clinical Cases in Mineral and Bone Metabolism* 12.2 (2015): 188.

Martin, Paul, and S. Joseph Leibovich. "Inflammatory cells during wound repair: the good, the bad and the ugly." *Trends in cell biology* 15.11 (2005): 599-607.

McIlwain, David R., Thorsten Berger, and Tak W. Mak. "Caspase functions in cell death and disease." *Cold Spring Harbor perspectives in biology* 5.4 (2013): a008656.

Mikolay, André, et al. "Survival of bacteria on metallic copper surfaces in a hospital trial." *Applied microbiology and biotechnology* 87.5 (2010): 1875-1879.

Mikulski, Damian, and Marcin Molski. "Quantitative structure–antioxidant activity relationship of trans-resveratrol oligomers, trans-4, 4'-dihydroxystilbene dimer, trans-resveratrol-3-O-glucuronide, glucosides: Trans-piceid, cis-piceid, trans-astringin and trans-resveratrol-4'-O-β-D-

glucopyranoside." *European journal of medicinal chemistry* 45.6 (2010): 2366-2380.

Mitchell, Simon, Jesse Vargas, and Alexander Hoffmann. "Signaling via the NF κ B system." *Wiley Interdisciplinary Reviews: Systems Biology and Medicine* 8.3 (2016): 227-241.

Mocchegiani, Eugenio, et al. "Micronutrient (Zn, Cu, Fe)–gene interactions in ageing and inflammatory age-related diseases: implications for treatments." *Ageing research reviews* 11.2 (2012): 297-319.

Mocchegiani, Eugenio, et al. "Micronutrient–gene interactions related to inflammatory/immune response and antioxidant activity in ageing and inflammation. A systematic review." *Mechanisms of ageing and development* 136 (2014): 29-49.

Morgan, Michael J., and Zheng-gang Liu. "Reactive oxygen species in TNF α -induced signaling and cell death." *Molecules and cells* 30.1 (2010): 1-12.

Mosser, David M., and Xia Zhang. "Interleukin-10: new perspectives on an old cytokine." *Immunological reviews* 226.1 (2008): 205-218.

Nicolson, Teresa. "The genetics of hair-cell function in zebrafish." *Journal of neurogenetics* 31.3 (2017): 102-112.

Novoa, Beatriz, and Antonio Figueras. "Zebrafish: model for the study of inflammation and the innate immune response to infectious diseases." *Current topics in innate immunity II*. Springer, New York, NY, 2012. 253-275.

Nguyen, Thanh Ngoc, et al. "Atg8 family LC3/GABARAP proteins are crucial for autophagosome–lysosome fusion but not autophagosome formation during PINK1/Parkin mitophagy and starvation." *J Cell Biol* 215.6 (2016): 857-874.

Nunez, Viviana A., et al. "Postembryonic development of the posterior lateral line in the zebrafish." *Evolution & development* 11.4 (2009): 391-404.

Pal, Amit. "Copper toxicity induced hepatocerebral and neurodegenerative diseases: an urgent need for prognostic biomarkers." *Neurotoxicology* 40 (2014): 97-101.

Pallepati, P., and D. A. Averill-Bates. "Reactive oxygen species, cell death signaling and apoptosis." *Princ Free Rad Biomed* 2 (2012): 513-546.

Pandey, Kanti Bhooshan, and Syed Ibrahim Rizvi. "Plant polyphenols as dietary antioxidants in human health and disease." *Oxidative medicine and cellular longevity* 2.5 (2009): 270-278.

Pantopoulos, Kostas, et al. "Mechanisms of mammalian iron homeostasis." *Biochemistry* 51.29 (2012): 5705-5724.

Papinski, Daniel, and Claudine Kraft. "Regulation of autophagy by signaling through the Atg1/ULK1 complex." *Journal of molecular biology* 428.9 (2016): 1725-1741.

Pardal, David, et al. "Resveratrol and piceid metabolites and their fat-reduction effects in zebrafish larvae." *Zebrafish* 11.1 (2014): 32-40.

Parichy, David M., et al. "Normal table of postembryonic zebrafish development: staging by externally visible anatomy of the living fish." *Developmental dynamics* 238.12 (2009): 2975-3015.

Porta, Camillo, Chiara Paglino, and Alessandra Mosca. "Targeting PI3K/Akt/mTOR signaling in cancer." *Frontiers in oncology* 4 (2014): 64.

Prasad, Rajendra, and Sandeep Kumar. "2. Biochemistry, molecular biology and molecular genetics of Wilson disease."

Rabanal-Ruiz, Yoana, Elsje G. Otten, and Viktor I. Korolchuk. "mTORC1 as the main gateway to autophagy." *Essays in biochemistry* 61.6 (2017): 565-584.

Radi, Rafael, et al. "Roles of catalase and cytochrome c in hydroperoxide-dependent lipid peroxidation and chemiluminescence in rat heart and kidney mitochondria." *Free Radical Biology and Medicine* 15.6 (1993): 653-659.

Ravagnan, Giampietro, et al. "Polydatin, a natural precursor of resveratrol, induces β -defensin production and reduces inflammatory response." *Inflammation* 36.1 (2013): 26-34.

Romero, Alejandro, et al. "A review of metal-catalyzed molecular damage: protection by melatonin." *Journal of Pineal Research* 56.4 (2014): 343-370.

Sabers, Candace J., et al. "Isolation of a protein target of the FKBP12-rapamycin complex in mammalian cells." *Journal of Biological Chemistry* 270.2 (1995): 815-822.

Sarkar, Sovan. "Regulation of autophagy by mTOR-dependent and mTOR-independent pathways: autophagy dysfunction in neurodegenerative diseases and therapeutic application of autophagy enhancers." (2013): 1103-1130.

Scheiber, Ivo, Ralf Dringen, and Julian FB Mercer. "Copper: effects of deficiency and overload." *Interrelations between essential metal ions and human diseases*. Springer, Dordrecht, 2013. 359-387.

Shalini, Sonia, et al. "Old, new and emerging functions of caspases." *Cell death and differentiation* 22.4 (2015): 526.

Simonetti, Rajla Bressan, et al. "Zebrafish (*Danio rerio*): The future of animal model in biomedical research." *Journal of Fisheries Sciences. com* 9.3 (2015): 39.

Şöhretoğlu, Didem, et al. "Recent advances in chemistry, therapeutic properties and sources of polydatin." *Phytochemistry reviews* 17.5 (2018): 973-1005.

Sonnack, Laura, et al. "Comparative analysis of the transcriptome responses of zebrafish embryos after exposure to low concentrations of cadmium, cobalt and copper." *Comparative Biochemistry and Physiology Part D: Genomics and Proteomics* 25 (2018): 99-108.

Steiner, Aaron B., et al. "Dynamic gene expression by putative hair-cell progenitors during regeneration in the zebrafish lateral line." *Proceedings of the National Academy of Sciences* 111.14 (2014): E1393-E1401.

Sun, Daekyu, et al. "Facilitation of a structural transition in the polypurine/polypyrimidine tract within the proximal promoter region of the human VEGF gene by the presence of potassium and G-quadruplex-interactive agents." *Nucleic acids research* 33.18 (2005): 6070-6080.

Tan, Qihua, Torben A. Kruse, and Kaare Christensen. "Design and analysis in genetic studies of human ageing and longevity." *Ageing Research Reviews* 5.4 (2006): 371-387.

Targos, Berenika, Jolanta Baranska, and Paweł Pomorski. "Store-operated calcium entry in physiology and pathology of mammalian cells." *ACTA BIOCHIMICA POLONICA-ENGLISH EDITION*- 52.2 (2005): 397.

Tisato, Francesco, et al. "Copper in diseases and treatments, and copper-based anticancer strategies." *Medicinal research reviews* 30.4 (2010): 708-749.

Turner, Mark D., et al. "Cytokines and chemokines: at the crossroads of cell signalling and inflammatory disease." *Biochimica et Biophysica Acta (BBA)-Molecular Cell Research* 1843.11 (2014): 2563-2582.

Vaillant, Angel A. Justiz, and Ahmad Qurie. "Immunodeficiency." *StatPearls [Internet]*. StatPearls Publishing, 2019.

- Varga, Máté, et al. "Autophagy is required for zebrafish caudal fin regeneration." *Cell death and differentiation* 21.4 (2014): 547.
- Vian, M. Abert, et al. "Simple and rapid method for cis-and trans-resveratrol and piceid isomers determination in wine by high-performance liquid chromatography using Chromolith columns." *Journal of chromatography A* 1085.2 (2005): 224-229.
- Wang, Hui-Lin, et al. "Comparative studies of polydatin and resveratrol on mutual transformation and antioxidative effect in vivo." *Phytomedicine* 22.5 (2015): 553-559.
- Wibowo, Indra, et al. "Compartmentalized Notch signaling sustains epithelial mirror symmetry." *Development* 138.6 (2011): 1143-1152.
- Willett, Catherine E., et al. "Early hematopoiesis and developing lymphoid organs in the zebrafish." *Developmental dynamics: an official publication of the American Association of Anatomists* 214.4 (1999): 323-336.
- Williams, J. A., and N. Holder. "Cell turnover in neuromasts of zebrafish larvae." *Hearing research* 143.1-2 (2000): 171-181.
- Xiao, Hai-tao, et al. "Membrane permeability-guided identification of neuroprotective components from *Polygonum cuspidatum*." *Pharmaceutical biology* 52.3 (2014): 356-361.
- Xu, C. Y., et al. "Effect of polydatin on learning and memory and expression of NR2B in the prefrontal cortex of rats with chronic alcoholism." *Zhongguo ying yong sheng li xue za zhi= Zhongguo yingyong shenglixue zazhi= Chinese journal of applied physiology* 27.2 (2011): 213-4.
- Xu, C. Y., et al. "Effect of polydatin on expression of cdk5 in the prefrontal cortex of rats with chronic alcoholism." *Zhongguo ying yong sheng li xue za zhi= Zhongguo yingyong shenglixue zazhi= Chinese journal of applied physiology* 28.2 (2012): 158-9.
- Zhang, L., and Z. P. Lv. "Effect of polydatin on nonalcoholic fatty liver disease and the TNF-a level in serum." *LiShizhen Med Mater Med Res* 21 (2010): 1007-8.
- Zhang, D. Q., L. S. Sun, and J. P. Xu. "Effect of piceid on the dog with an acute myocardial infarction model." *Herald Med (Chin)* 25 (2006): 510-513.

Zhang, Ting, et al. "Transcriptional responses and mechanisms of copper-induced dysfunctional locomotor behavior in zebrafish embryos." *Toxicological sciences* 148.1 (2015): 299-310.

Zhao J, Li HY, Wang ZH, et al. "Effect of polydatin on ultrastructure of cardiac myocytes in rats with adriamycin-induced myocardial damage" *Acta Acad Med* 30.634 (2010): 19-629.

Zhao, Lu, Zhidan Xia, and Fudi Wang. "Zebrafish in the sea of mineral (iron, zinc, and copper) metabolism." *Frontiers in pharmacology* 5 (2014): 33.

Index of figure and table

Fig.1.1 Females and male zebrafish (www.asianscientist.com).....	2
Fig.1.2 Posterior lateral line neuromasts at 3dpf (Chitnis et al., 2012).....	7
Fig.1.3 Neuromast structure (Ghysen and Dambly-Chaudière, 2004).	8
Fig.1.4 <i>Polygonum cuspidatum</i> (www.zeauniverse.com).....	10
Fig.1.5 Chemical structures of the different classes of polyphenols (Pandey and Rizvi, 2009).....	11
Fig.1.6 Resveratrol and polydatin cis and trans conformations (Vian et al., 2005).....	12
Fig.1.7 Biological properties of PLD (Şöhretoğlu et al., 2018).....	14
Fig.1.8 Copper metabolism (Rajendra Prasad and Sandeep Kumar, 2013).....	20
Fig.1.9 NF-kB Family (www.creative-diagnostics.com).....	23
Fig.1.10 <i>mtor</i> and autophagy related gene signaling (Rabanal-Ruiz et al., 2017).....	26
Fig.3.1 Experimental design with copper exposure. The abbreviations as in text mean PD=polydatin, T0=72hpf, T1=75hpf, T2=77hpf, T3=78hpf, T4=102hpf, T5=126hpf.....	40
Fig.3.2 Experimental design with cut tail. The abbreviations as in text mean PD=polydatin, T0=72hpf, T1=75hpf, T2=77hpf, T3=78hpf.....	43

Fig.3.3 Experimental design polydatin timing test. The abbreviations as in text mean PD=polydatin, t0=72hpf, t1=74hpf, t2=75hpf, t3=77hpf, t4=78hp.....47

Fig.3.4 Electrophoresis run of 4 samples (2 from control group and 2 from CuSO₄ group).....53

Table 3.1 The table shows forward and reverse primers sequences and primer Melting Temperature (Tm) for each analyzed gene.....56

Fig.4.1 Rappresentative picture of zebrafish larvae, sampling at T5, exposed to copper sulphate and polydatin treatments (Scale 1000µm). Black arrows indicate the presence of the swim bladder while white arrow spinal cord curvature.....58

Fig.4.2 Figure show the lengths (mm) of larvae sampled at T4 (a) and T5 (b), letters indicate significant differences (p<0.05) and the growth in length of the larvae between T4 and T5 sampling time (c). In c asterisks indicate significant differences in length between larvae sampled at T4 and larvae sampled at T5, while letters indicate differences in larvae growth between various experimental groups (p <0.05).....59

Fig.4.3 The figure shows the percentage of larvae with correct swim bladder insufflation at T5.....61

Fig.4.4 The graph shows the percentage of larvae with a dorsal curvature at T5.....62

Fig.4.5 Figure shows representative images of neutrophils presence in the head of the control group larvae (CTRL) and larvae treated with copper sulphate and sampled respectively: one hour after the exposure end (CuSO₄ 1hpe), 3 hours

from exposure end (CuSO₄ 3hpe) and 6 hours after exposure end (CuSO₄ 6hpe). Black arrows indicate neutrophils. Scale 100µm.....63

Fig.4.6.a. The figure shows representative images of neutrophil migration in the head of the larvae. Photos represent the four experimental groups: control group larvae (CTRL), larvae treated only with copper sulfate (CuSO₄), larvae treated with polydatin for 3 hours before copper exposure (PD-t0 + CuSO₄-t2) and larvae treated with polydatin for 1 hour before copper exposure (PD-t1+CuSO₄-t2). Neutrophils are indicated with black arrows. Scale 100µm.....64

Fig.4.6.b The figure shows representative images of neutrophil migration in larvae lateral line. Photos represent the four experimental groups: control group larvae (CTRL), larvae treated only with copper sulfate (CuSO₄), larvae treated with polydatin for 3 hours before copper exposure (PD-t0 + CuSO₄-t2) and larvae treated with polydatin for 1 hour before copper exposure (PD-t1+CuSO₄-t2). In the lower center there is a larva in its entirety which indicates the portion on which we have concentrated to capture the images of the lateral line. Neutrophils are indicated by black arrow. Scale 50µm.....65

Fig.4.7.a The figure shows representative images of neutrophil migration in the head of larvae sampled at T3. Photos represent the 6 experimental groups: control larvae (CTRL), larvae treated only with copper sulfate (CuSO₄), larvae treated with polydatin alone (PD-T0 and PD-T2), larvae treated with polydatin before copper exposure (PD+CuSO₄) and larvae treated with polydatin after copper exposure (CuSO₄+PD). Neutrophils are indicated with black arrows. Scale 100 µm.....67

Fig.4.7.b The figure shows representative images of neutrophil migration in lateral line of larvae sampled at T3. Photos represent the 6 experimental groups: control larvae (CTRL), larvae treated only with copper sulfate (CuSO₄), larvae treated with polydatin alone (PD-T0 and PD-T2), larvae treated with polydatin before copper exposure (PD+CuSO₄) and larvae treated with polydatin after copper exposure (CuSO₄+PD). In the lower center there is a larva in its entirety which indicates the portion on which we have concentrated to capture the images of the lateral line. Neutrophils are indicated with black arrows. Scale 50 μm.....68

Fig.4.8 The figure shows representative images of neutrophil migration in caudal fin of larvae sampled at T3. Photos represent 6 experimental groups: control larvae (CTRL), larvae that have had an incision of the caudal fin(TAIL CUT), larvae treated with polydatin alone (PD-T0 and PD-T2), larvae treated with polydatin before caudal fin incision (PD+TAIL CUT) and larvae treated with polydatin after caudal fin incision (TAIL CUT+PD). Neutrophils are indicated with black arrows. Scale 100 μm.....70

Fig.4.9 Picture shows lateral line neuromast (in fluorescence) in larvae sampled at time T3. The photos represent the 6 experimental groups: control larvae (CTRL), larvae treated only with copper sulfate (CuSO₄), larvae treated with polydatin alone (PD-T0 and PD-T2), larvae treated with polydatin before copper exposure (PD+CuSO₄) and larvae treated with polydatin after copper exposure (CuSO₄+PD). Scale 500 μm.....71

Fig.4.10 DASPEI staining high magnification of L1 neuromast (in fluorescence) in larvae sampled at time T3 (top line) and T4(lower line). Photos represent the 6 experimental groups from left to right: control larvae (CTRL), larvae treated only with copper sulfate (CuSO₄), larvae treated with polydatin

alone (PD-T0 and PD-T2), larvae treated with polydatin before copper exposure (PD-T0+CuSO₄-T1) and larvae treated with polydatin after copper exposure (CuSO₄+PD-T2). Scale 5 μm.....72

Fig.4.11 Relative mRNA abundance of *ill* (a), *il8* (b) and *ill0* (c) in 6 experimental groups: control larvae (CTRL), larvae treated only with copper sulphate (CuSO₄), larvae treated with polydatin alone (PD-T0 and PD-T2), larvae treated with polydatin before copper exposure (PD+CuSO₄) and larvae treated with polydatin after copper exposure (CuSO₄+PD). Letters indicate significant differences (p <0.05).....73

Fig.4.12 Relative mRNA abundance of *sod1* (a), *sod2* (b) and *cat* (c) in 6 experimental groups: control larvae (CTRL), larvae treated only with copper sulphate (CuSO₄), larvae treated with polydatin alone (PD-T0 and PD-T2), larvae treated with polydatin before copper exposure (PD+CuSO₄) and larvae treated with polydatin after copper exposure (CuSO₄+PD). Letters indicate significant differences (p <0.05).....75

Fig.4.13 Relative mRNA abundance of *mtor* in 6 experimental groups: control larvae (CTRL), larvae treated only with copper sulphate (CuSO₄), larvae treated with polydatin alone (PD-T0 and PD-T2), larvae treated with polydatin before copper exposure (PD+CuSO₄) and larvae treated with polydatin after copper exposure (CuSO₄+PD). Letters indicate significant differences (p <0.05).....77

Fig.4.14 Relative mRNA abundance of *casp3* (a) and *p53* (b) in 6 experimental groups: control larvae (CTRL), larvae treated only with copper sulphate (CuSO₄), larvae treated with polydatin alone (PD-T0 and PD-T2), larvae treated with polydatin before copper exposure (PD+CuSO₄) and larvae treated

with polydatin after copper exposure (CuSO₄+PD). Letters indicate significant differences (p <0.05).....78

Fig.4.15 Relative mRNA abundance of *ambra1* (a) and *lc3* (b) in 6 experimental groups: control larvae (CTRL), larvae treated only with copper sulphate (CuSO₄), larvae treated with polydatin alone (PD-T0 and PD-T2), larvae treated with polydatin before copper exposure (PD+CuSO₄) and larvae treated with polydatin after copper exposure (CuSO₄+PD). Letters indicate significant differences (p <0.05).....79

Fig.4.16 Relative mRNA abundance of *cldn b* (a) and *phoenix* (b) in 6 experimental groups: control larvae (CTRL), larvae treated only with copper sulphate (CuSO₄), larvae treated with polydatin alone (PD-T0 and PD-T2), larvae treated with polydatin before copper exposure (PD+CuSO₄) and larvae treated with polydatin after copper exposure (CuSO₄+PD). Letters indicate significant differences (p <0.05).....80

Fig.4.17 Relative mRNA abundance of *cyclin b* (a) and *ccna2* (b) in 6 experimental groups: control larvae (CTRL), larvae treated only with copper sulphate (CuSO₄), larvae treated with polydatin alone (PD-T0 and PD-T2), larvae treated with polydatin before copper exposure (PD+CuSO₄) and larvae treated with polydatin after copper exposure (CuSO₄+PD). Letters indicate significant differences (p <0.05).....82

RINGRAZIAMENTI

Prima di iniziare questo percorso mai, e dico mai, avrei pensato di avere le capacità, la determinazione e la tenacia per portare avanti un progetto del genere. Eppure, eccomi qua, al termine di questo meraviglioso viaggio, a ringraziare chi ha permesso tutto ciò e chi mi è stato accanto in qualsiasi circostanza.

Ringrazio il mio relatore, la Prof.ssa Oliana Carnevali, innanzitutto per avermi dato la possibilità di prendere parte ad un progetto meraviglioso ed interessante come questo che mi ha permesso di imparare e scoprire tantissime cose nuove. Ma la ringrazio davvero dal profondo del cuore per la fiducia che mi ha dato, per aver creduto in me e per avermi sempre incoraggiata. Non ci sono parole per descrivere quanto le sia grata per tutto ciò.

Si ringrazia il gruppo di ricerca del Dipartimento di Patologia Clinica e Terapia Innovativa dell'Italian National Research Center for Aging, INRCA-IRCCS per la collaborazione e per la disponibilità al confronto dal quale è nata l'idea di utilizzare la polidatina come agente antiossidante e per la fornitura della stessa.

Si ringrazia la Prof.ssa Luisa Dalla Valle del Dipartimento di Biologia dell'Università di Padova per i consigli dati sulla messa a punto del piano sperimentale.

Ringrazio la Prof.ssa Giorgia Gioacchini, la Prof.ssa Francesca Maradonna e il Prof. Ike Olivotto per l'enorme aiuto e gli insegnamenti che mi hanno dato durante questo percorso.

Ringrazio il mio correlatore, Andrea, per il supporto e i consigli che mi ha dato in questi ultimi mesi di lavoro. Ma soprattutto grazie per la pazienza, la gentilezza e l'umanità dimostrata sin dal primo momento; sono sicura che sarai un papà meraviglioso, Francesco Leonida è un bambino molto fortunato.

Ringrazio Basilio per l'aiuto, gli input e il sostegno ricevuto in questo percorso. Da te ho imparato moltissime cose. Grazie per esserci stato sempre e per aver creduto in me.

Ringrazio Andrea Z., Arturo, Chiara, Danilo, Jerry, Luca, Matteo, Michela e Valentina per la grande disponibilità e professionalità dimostrata e per avermi sempre dato una mano ogni volta che ne ho avuto bisogno.

Ringrazio Martina per avermi guidata durante i primi mesi di questo percorso.

Ringrazio la mia coinquilina Maria Vittoria, per avermi sopportata e supportata in tutti questi anni, e in particolar modo durante questo percorso così intenso della mia vita. Grazie per essermi sempre stata accanto, per aver pianto e gioito con me. I momenti passati insieme resteranno nel mio cuore per sempre.

Ringrazio tutti i miei amici, vicini e lontani. Ognuno di voi ha reso la mia vita più ricca e speciale. Grazie per l'incoraggiamento e l'aiuto che mi avete dato sempre.

Ringrazio tutti i miei amici volontari CRI e in modo particolare il gruppo Giovani del Comitato di Ancona per il sostegno in questo percorso. Il volontariato mi ha dato tanto, la gioia nel ricevere un semplice grazie è qualcosa di indescrivibile. La Croce Rossa, con i suoi sette principi e le sue mille sfaccettature mi ha permesso di crescere, di aprire la mente, di maturare e mi ha spinto a fare del mio meglio. Non potrei mai più immaginare la mia vita senza tutto ciò. Grazie.

Durante questo percorso ho imparato che in genere, negli articoli scientifici, l'ultimo nome nell'ordine degli autori dell'articolo è quello del capo, ossia della persona più importante del gruppo di ricerca. Per questo motivo, in ultimo, voglio ringraziare la mia famiglia, le persone più importanti della mia vita.

Ringrazio tutti i miei cuginetti, Giulia, Martina, Matteo, Matteo e Michele, e in particolare Alessia, la mia figlioccia, per aver sempre creduto in me. Spero di essere un ottimo esempio per voi e vi auguro che nella vita possiate ottenere tutto ciò che desiderate, ma soprattutto spero che siate sempre felici.

Ringrazio tutti i miei zii, per avermi sempre coccolata sin da quando ero piccola. L'affetto che ho ricevuto da ognuno di voi è stato immenso. Avete sempre creduto in me e mi avete sempre incoraggiata. Grazie di cuore per tutto.

Ringrazio i miei nonni Arcangela, Maria e Matteo per tutto l'amore che mi avete dato da sempre. Spero che oggi siate orgogliosi di me. Questo traguardo è per voi.

Caro nonno, oggi più che mai, avrei voluto tu fossi qui, a festeggiare questa vittoria con me. Spero che anche da lassù tu possa essere orgoglioso di me. Da sempre volevi che diventassi Dottoressa, beh, oggi lo sono, una dottoressa diversa magari da quella che intendevi dire tu, ma è quello che mi rende felice, e sono sicura che se sono felice io, lo sei anche tu. Mi manchi moltissimo.

Ringrazio Michele, mio fratello, da quando sei arrivato tu la mia vita è cambiata, non mi sono sentita più sola e hai sempre rallegrato le mie giornate. Ogni giorno che passa sono sempre più orgogliosa dell'uomo che stai diventando. Ti auguro che dalla vita tu possa ottenere tutto ciò che desideri. Vedrai che l'impegno, la tenacia e l'onestà ti porteranno dove vuoi tu, basta crederci e fare sempre del proprio meglio. Ti voglio bene.

Ringrazio infine i miei genitori. La mia vita. A voi devo tutto, tutto ciò che sono, tutto ciò che ho lo devo a voi ed al vostro amore per me. Grazie per avermi dato la possibilità di portare a termine questo percorso di studi, ma soprattutto grazie per avermi sempre supportata in qualsiasi circostanza, per avermi sempre aiutato a rialzarmi ogni volta che sono caduta e per avermi incoraggiata a fare del mio meglio da sempre. Sono la figlia più fortunata

del mondo ad avere dei genitori come voi. Ringraziarvi non sarà mai abbastanza, ma spero siate orgogliosi di me, per il mio traguardo, ma soprattutto per la persona che sono diventata. Vi amo.

Concludo nella speranza di non aver dimenticato nessuno. Sono davvero tante le persone che ho incontrato nella mia vita e ognuna di loro in un modo o nell'altro mi ha resa ciò che sono oggi. Ormai sono giunta alla fine di questo percorso, che in realtà segna semplicemente un nuovo inizio. Non nego che il futuro mi spaventi un po', ma spero di riuscire a cavarmela come ho sempre fatto. È ora di spiccare il volo.

Per aspera ad astra

Mery

